ESAIM: M2AN 58 (2024) 157–189
https://doi.org/10.1051/m2an/2023099
ESAIM: Mathematical Modelling and Numerical Analysis
www.esaim-m2an.org

A MIXED PARAMETER FORMULATION WITH APPLICATIONS TO LINEAR VISCOELASTIC SLENDER STRUCTURES

Erwin Hernández[1], Felipe Lepe[2] and Jesus Vellojin[2,*]

Abstract. We present the analysis of an abstract parameter-dependent mixed variational formulation based on Volterra integrals of second kind. Adapting the classic mixed theory in the Volterra equations setting, we prove the well posedness of the resulting system. Stability and error estimates are derived, where all the estimates are uniform with respect to the perturbation parameter. We provide applications of the developed analysis for a viscoelastic Timoshenko beam and report numerical tests for this problem. We also comment, numerically, the performance of a viscoelastic Reissner–Mindlin plate.

Mathematics Subject Classification. 65M12, 65M60, 35Q74, 45D05, 65R20, 65N12, 74D05.

Received December 6, 2022. Accepted December 3, 2023.

1. Introduction

Viscoelasticity is a physical property, presented in a wide variety of structures and became important after the popularization of polymers. The study of viscoelastic materials, their damping capacity and behavior in time due to induced stress or temperature changes, is well established and we refer to the studies of Flugge [20], Christensen [15] and Reddy [43] for a rigorous theoretical development.

There are several mathematical models and numerical methods to approximate the solutions of viscoelastic problems. In particular, the finite difference method and the finite element method are the usual numerical tools that mathematicians and engineers implement in order to compute, with high accuracy, the viscoelastic response of some materials. We refer to [3, 12, 29, 49] as papers that analyze these subjects.

An important subject of study in engineering is the one associated to slender structures. These elements are often modeled by systems of partial differential equations where the thickness is considered on the model as a parameter (see, for instance, [10]). This parameter takes importance on the elastic response of the structures. Moreover, from the numerical methods point of view, it is well known that when the thickness of some structure is smaller than the rest of the dimensions, difficulties in the convergence of such methods arise, leading to the so-called locking phenomenon. There is an extensive amount of studies where this numerical phenomenon has been studied in order to provide robust numerical methods that approximate the corresponding solutions independently of the parameters that may lead to locking, such as those in [4, 7, 9, 13, 21, 26, 31, 32] where reduced integration and mixed formulations have been considered. Also, locking free numerical methods have emerged

Keywords and phrases. Viscoelasticity, Volterra integrals, mixed methods, locking-free, error estimates.

[1] Departamento de Matemática, Universidad Técnica Federico Santa María, Casilla 110-V Valparaiso, Chile.

[2] GIMNAP-Departamento de Matemática, Universidad del Bío-Bío, Casilla 5-C, Concepción, Chile.

*Corresponding author: `jvellojin@ubiobio.cl`

for vibration, buckling, and spectral problems as [33,35,36], showing accurate results when the eigenvalues and eigenfunctions are approximated.

This drawback that arises in elliptic models with no memory terms, can be also found in the context of Volterra systems such as viscoelastic structures, as is presented, for instance, in [27,28]. The aforementioned references leads to the natural question that if is possible to consider mixed formulations for viscoelastic materials, knowing that in the elastic setting the locking phenomenon is avoided. In particular, we focus our interest in slender and moderate thin structures where the thickness plays an important role in the robustness of the proposed numerical methods. The resulting parameter dependent problem needs to be analyzed rigorously in order to prove that the proposed numerical method is stable with respect to the thickness. Let us mention that, our contribution is focused on the study of conforming methods and thin structures as a key stone for other type of memory problems involving fluids, coupled problems, etc.

One of the most commonly used mathematical tools to address parameter-dependent problems are mixed formulations with a perturbation parameter. If λ is this parameter, a mixed formulation associated to it read as: Find $(u,p)\in\mathcal{V}\times\mathcal{Q}$ such that

$$\begin{cases} a(u,v)+b(v,p)=\langle f,v\rangle_{\mathcal{V}},\\ b(u,q)-\lambda(p,q)_{\mathcal{Q}}=\langle g,q\rangle_{\mathcal{Q}},\end{cases}$$

where $a:\mathcal{V}\times\mathcal{V}\to\mathbb{R}$, $b:\mathcal{V}\times\mathcal{Q}\to\mathbb{R}$ are two bilinear forms, $\langle\cdot,\cdot\rangle_{\mathcal{V}}$ and $\langle\cdot,\cdot\rangle_{\mathcal{Q}}$ the duality pairing between the spaces $\mathcal{V}$ and $\mathcal{V}'$ and $\mathcal{Q}$ and $\mathcal{Q}'$, respectively, and $(\cdot,\cdot)_{\mathcal{Q}}$ is the corresponding inner product in $\mathcal{Q}$. The theory behind this formulation is rich and extensive for Hilbert spaces, and we refer to [8] as a classic reference about this subject. On the other hand there is the theory of Volterra integrals, which has allowed the study of evolutionary problems where a memory term is presented, widely used in viscoelasticity models obtained by means of the Boltzmann superposition principle. In this work we consider both theories in order to study the following mixed formulation with Volterra integral equations:

Problem 1.1. Given $1\leq\ell\leq\infty$, $f\in L^{\ell}(\mathcal{J};\mathcal{V}')$ and $g\in L^{\ell}(\mathcal{J};\mathcal{Q}')$, find $(u,p)\in L^{\ell}(\mathcal{J};\mathcal{V}\times\mathcal{Q})$ such that

$$\begin{cases} a(u(t),v)+b(v,p(t))=\langle f(t),v\rangle_{\mathcal{V}}+\displaystyle\int_0^t\Big[\widetilde{a}(t,s;(u(s),v))+\widetilde{b}(t,s;(v,p(s)))\Big]\,\mathrm{d}s,\\ b(u(t),q)-\lambda(p(t),q)_{\mathcal{Q}}=\langle g(t),q\rangle_{\mathcal{Q}},\end{cases}$$

for all $(v,q)\in\mathcal{V}\times\mathcal{Q}$.

For this model, $\mathcal{V}$ and $\mathcal{Q}$ represent suitable spaces satisfying some prescribed boundary conditions, $\mathcal{J}:=[0,T]$, $T\in(0,\infty)$, represents a period of observation. The new *time-dependent* forms (bilinear forms in space) $\widetilde{a}:\mathcal{T}\times\mathcal{V}\times\mathcal{V}$ and $\widetilde{b}:\mathcal{T}\times\mathcal{V}\times\mathcal{Q}$, with $\mathcal{T}:=\{(s,t)\in\mathcal{J}\times\mathcal{J}\mid 0\leq s\leq t\}$, take the role of memory term contributions. The specific form of these bilinear forms is directly related to the Volterra kernel, and may acquire a nonlinear nature in some cases. However, our work is based on the application of this model to linear viscoelasticity, so there will be a *similarity* between them and the bilinear forms $a(\cdot,\cdot)$ and $b(\cdot,\cdot)$ (see for example [46] for a primal formulation and Sect. 2 below). For simplicity, we will only write the time dependence on the unknowns when it is strictly necessary.

In this formulation, the typical features of both theories such as ellipticity of $a(\cdot,\cdot)$ in the kernel of $b(\cdot,\cdot)$, an inf-sup condition of $b(\cdot,\cdot)$, L^1 continuity of the Volterra kernel, or long term behavior, can be considered. Our work will focus on characterizing estimates of this model in order to be applied in viscoelastic slender structures, considering a short-term behavior, and standard hypotheses of elastic problems.

The paper also propose an abstract framework to analyze a mixed formulation of a viscoelastic model, which is capable to guarantee the stability for the viscoelastic system, as in the classic elasticity approach, but with the addition of ℓ-regularity in time. Let us remark that the proposed study is also directed for the analysis of numerical methods, more precisely, conforming finite element methods to approximate the solution of viscoelastic systems in mixed form. The consideration of non-conforming schemes will be considered in future studies. To make matters precise, our model can be considered as an extension to viscoelasticity of the well-known regular and penalty type cases in elasticity (see [4, 27, 28] for instance). Moreover, the numerical experiments in this work show that the spatial convergence is not affected by a particular choice of ℓ. Note that since our abstract framework is quasi-static, the initial conditions are not needed.

It is well known that mixed formulations avoid the locking phenomenon that arises due some parameter (or parameters) present in the models [8]. This is the case of viscoelastic slender structures. For instance, in the work of [44], a weak symmetry formulation is considered that leads to a mixed formulation in linear viscoelasticity for solids, that is capable of avoid locking. The authors use constitutive equations in differential operator form, where the models are associated with Maxwell and Kelvin–Voigt materials. Recently, a new approach to deal with the numerical locking-free approximation of thin viscoelastic shells has been introduced in [28], where the authors had obtained a new viscoelastic shell formulation, based in the mixed formulation of pure elastic shell in [10]. Another approach for non-uniform viscoelastic Timoshenko beams presented in [27]. Here, the authors explore the analysis on a geometrically non-uniform linear viscoelastic Timoshenko beam by means of a penalized mixed formulation. The error estimates are obtained for $\ell = 1$. There is also the corresponding principle, that allows to translate the viscoelastic problem into an equivalent elastic one, for which locking-free numerical methods can be applied. Although this approach is useful to compute exact solutions, it has several drawbacks since it depends on the time invariance of the boundary conditions and the nature of the relaxation modulus [40].

Also, our formulation is different from those proposed in other works (for example [18, 30, 48]) that consider mixed formulations with memory, and can be considered as an extension of [27]. This is because the presence of the perturbation parameter, whose presence changes the rules of the game. Here, one of the main difficulties will be to obtain a well-posed problem, such that the estimates do not deteriorate as the perturbation parameter becomes small. The aforementioned problem in viscoelasticity is expectable, and hence, numerical methods can be affected by the locking phenomenon as well. This will be the major contribution of this study, whose versatility can be extended to the study of systems with dissipative or inertia terms, depending on the phenomenon under study.

The paper is organized as follows: In Section 2 we introduce an abstract setting in which we will operate through our paper. We also provide stability bounds, independent of the perturbation parameter. In Section 3 we present the analysis of a semi-discrete scheme of the continuous problem that takes into account several common discrete spatial assumptions such as conforming finite element spaces or semi-discrete inf-sup conditions. In Section 4 we apply our developed abstract framework to a Timoshenko beam, which fits in the theoretical framework that we develop. More precisely, this model presents a parameter associated to the thickness that, as is well established, produces locking for standard numerical schemes. Under the assumption of suitable spatial regularity, we derive error estimates for a standard family of finite elements, where the involved constants are uniform on the thickness. We also go beyond to the developed theory and consider the Reissner–Mindlin plate. This model, in contrast with the Timoshenko beam model, has a different perturbation nature and does not fit in the proposed framework, more precisely, is a singular perturbation problem. Despite of this theoretical fact, we implement the classic Durán–Liberman elements to discretize the plate model in order to observe the good performance and accuracy of the proposed mixed finite element methods for the viscoelastic plate model.

2. The abstract setting

Let us fix some notations. Through all our manuscript the relation $\mathtt{a} \lesssim \mathtt{b}$ indicates $\mathtt{a} \leq C\mathtt{b}$, where C is a positive constant independent of $\mathtt{a}$ and $\mathtt{b}$. We denote by $\mathcal{V}$ and $\mathcal{Q}$ two Hilbert spaces endowed with the norms $\|\cdot\|_{\mathcal{V}}$ and $\|\cdot\|_{\mathcal{Q}}$, respectively. We denote by $\mathcal{L}(\mathcal{V};\mathcal{Q})$ the space of continuous linear mappings from $\mathcal{V}$ to $\mathcal{Q}$. Also, we denote by $\mathcal{V}'$ and $\mathcal{Q}'$ their corresponding dual spaces endowed with norms $\|\cdot\|_{\mathcal{V}'}$ and $\|\cdot\|_{\mathcal{Q}'}$. For every Banach space $\mathcal{B}$ and every time interval $[0,t]$, we denote by $L^{\ell}(0,t;\mathcal{B})$ the space of maps $\mathfrak{w} : [0,t] \to \mathcal{B}$ with norm, for $1 \leq \ell < \infty$,

$$\|\mathfrak{w}\|_{L^\ell(0,t;\mathcal{B})} := \left(\int_0^t \|\mathfrak{w}\|_{\mathcal{B}}^\ell\right)^{1/\ell},$$

with the obvious modification for $\ell = \infty$.

The integral equations are formulated in such a way that the spatial components are analyzed using results of mixed formulations. Here, and in the forthcoming sections, we will omit the time dependence of the solutions and test functions outside the time integral unless necessary in the arguments.

We recall that λ is a small parameter such that $0 < \lambda \leq \lambda_{\max} < \infty$. It is important to remark that in real applications this parameter is allowed to be significantly small.

Now we will introduce a series of hypotheses that are required to prove our results. Some of the results are classic in the mixed formulations literature [8].

Assumption 2.1. *Let us denote by $\mathbb{A} : \mathcal{V} \to \mathcal{V}'$ and $\mathbb{B} : \mathcal{V} \to \mathcal{Q}'$ the corresponding induced linear operators from the bilinear forms $a(\cdot,\cdot)$ and $b(\cdot,\cdot)$, respectively, and $\mathbb{B}^*$ the adjoint operator of $\mathbb{B}$. In the forthcoming analysis we denote the linear operators induced induced by $\widetilde{a}(\cdot,\cdot;(\cdot,\cdot))$ and $\widetilde{b}(\cdot,\cdot;(\cdot,\cdot))$ as $\widetilde{\mathbb{A}}$ and $\widetilde{\mathbb{B}}$, respectively. Moreover, given $\ell \in [1,\infty]$, we assume that:*

(i) *The bilinear form $a(\cdot,\cdot)$ is continuous, symmetric, positive semi-definite on $\mathcal{V} \times \mathcal{V}$, whereas $b(\cdot,\cdot)$ is a continuous bilinear form on $\mathcal{V} \times \mathcal{Q}$. Hence, it follows that*

$$\begin{aligned}|a(v,w)| &\leq \|\mathbb{A}\|_{\mathcal{L}(\mathcal{V};\mathcal{V}')}\|v\|_{\mathcal{V}}\|w\|_{\mathcal{V}} \equiv C\|v\|_{\mathcal{V}}\|w\|_{\mathcal{V}},\\ |b(v,q)| &\leq \|\mathbb{B}\|_{\mathcal{L}(\mathcal{V};\mathcal{Q}')}\|v\|_{\mathcal{V}}\|q\|_{\mathcal{Q}} \equiv C\|v\|_{\mathcal{V}}\|q\|_{\mathcal{Q}},\end{aligned}$$

for all $w, v \in \mathcal{V}$. Also, we have that

$$\begin{aligned}\langle \mathbb{A}w, v\rangle_{\mathcal{V}} &= \langle w, \mathbb{A}v\rangle_{\mathcal{V}} = a(w,v) \qquad \forall w, v \in \mathcal{V}.\\ \langle \mathbb{B}v, q\rangle_{\mathcal{Q}} &= \langle v, \mathbb{B}^*q\rangle_{\mathcal{V}} = b(v,q) \qquad \forall v \in \mathcal{V}, \quad \forall q \in \mathcal{Q}.\end{aligned}$$

For the operator $\mathbb{B}$, we set $\mathcal{K} := \ker \mathbb{B} \subset \mathcal{V}$.

(ii) *The operators $\widetilde{\mathbb{A}}(t,s)$, $\widetilde{\mathbb{B}}(t,s)$ and $\widetilde{\mathbb{B}}^*(t,s)$ are similar to $\mathbb{A}$, $\widetilde{\mathbb{B}}$ and $\mathbb{B}^*$, respectively, in the sense that there exist $\phi_a, \phi_b \in L^1(\mathcal{J};[0,\infty))$, such that (see for example [46], Sect. 1)*

$$\widetilde{\mathbb{A}}(t,s) := \phi_a(t-s)\mathbb{A}, \quad \widetilde{\mathbb{B}}(t,s) := \phi_b(t-s)\mathbb{B}, \quad \widetilde{\mathbb{B}}^*(t,s) := \phi_b(t-s)\mathbb{B}^*.$$

Moreover, it follows that

$$\begin{aligned}|\widetilde{a}(t,s,(w,v))| &\lesssim \phi_a(t-s)\,\|w\|_{\mathcal{V}}\|v\|_{\mathcal{V}},\\ |\widetilde{b}(t,s,(v,q))| &\lesssim \phi_b(t-s)\,\|v\|_{\mathcal{V}}\|q\|_{\mathcal{Q}},\end{aligned}$$

a.e in $\mathcal{T}$, for all $v, w \in \mathcal{V}$ and for all $q \in \mathcal{Q}$.

(iii) *We consider that $f \in L^\ell(\mathcal{J};\mathcal{V}')$ and $g \in L^\ell(\mathcal{J};\mathcal{Q}')$ are continuous in the sense that*

$$\begin{aligned}|\langle f, v\rangle_{\mathcal{V}}| &\leq \|f\|_{\mathcal{V}'}\|v\|_{\mathcal{V}} \qquad \forall v \in \mathcal{V},\\ |\langle g, q\rangle_{\mathcal{Q}}| &\leq \|g\|_{\mathcal{Q}'}\|q\|_{\mathcal{Q}} \qquad \forall q \in \mathcal{Q},\end{aligned}$$

a.e. in $\mathcal{J}$, for all $v \in \mathcal{V}$ and for all $q \in \mathcal{Q}$.

The system of operator equations associated to Problem 1.1 is the following:

Problem 2.2. Given $f \in L^\ell(\mathcal{J};\mathcal{V}')$ and $g \in L^\ell(\mathcal{J};\mathcal{Q}')$, find $(u,p) \in L^\ell(\mathcal{J};\mathcal{V} \times \mathcal{Q})$ such that

$$\begin{cases} \mathbb{A}u(t) + \mathbb{B}^*p(t) = f(t) + \displaystyle\int_0^t \left[\widetilde{\mathbb{A}}(t,s)u(s) + \widetilde{\mathbb{B}}^*(t,s)p(s)\right] \mathrm{d}s,\\ \mathbb{B}u(t) - \lambda\mathfrak{R}_{\mathcal{Q}}p(t) = g(t),\end{cases}$$

where $\mathfrak{R}_{\mathcal{Q}} : \mathcal{Q} \to \mathcal{Q}'$ is the Riesz operator.

In order to derive the main result of the present section, we recall some properties on Volterra equations which are necessary to obtain the stability of the solutions of Problem 1.1 (see [22, 23] for instance).

Definition 2.3 (Laplace-type convolution)**.** Let m and n be two integrable functions over $\mathcal{J}$. We denote the Laplace-type convolution between m and n by

$$(m * n)(t) := \int_0^t m(t-\tau)n(\tau)\,\mathrm{d}\tau.$$

Let us remark that the convolutions presented in this study are based on the Boltzmann superposition principle, which obeys the principle of Causality in the sense that the viscoelastic response at any point in time depends on the action at the instant, as well as on the complete history of its actions. For states prior to $t = 0$ it is assumed that there are no actions associated with the material response, whereas the assumption of a non-aging material guarantees that the material is homogeneous with respect to time. Thus the support of the integral is $(0, t)$. For more details we refer to Chapter 1 of [22] and Chapter 2 of [24].

In the following we provide a lemma that will be widely used through our work since it will allow us to establish estimates between L^1 and L^ℓ functions, for $\ell \in [1, \infty]$. The proof can be found in [46].

Lemma 2.4. *Let $m \in L^1(\mathcal{J})$ and $n \in L^\ell(\mathcal{J})$ for some $\ell \in [1, \infty]$. Then, the convolution $m * n$ belongs to $\in L^\ell(\mathcal{J})$ and the estimate*

$$\|m * n\|_{L^\ell(0,t)} \leq \|m\|_{L^1(0,t)}\|n\|_{L^\ell(0,t)},$$

holds, for all $t \in \mathcal{J}$. If $\ell = \infty$, then $m * n$ is a bounded uniformly continuous function on $\mathcal{J}$.

In the study of the integral equations throughout this paper, the application of the following Gronwall's inequality will play an important role.

Lemma 2.5 (Gronwall's inequality)**.** *Suppose that the functions $K(t) \geq 0$ and $F(t)$ are absolutely integrable, and the integrable function $v(t) \geq 0$ satisfies the following inequality*

$$v(t) \leq F(t) + \int_0^t K(s)v(s)\,\mathrm{d}s.$$

Then, it follows

$$v(t) \leq F(t) + \int_0^t K(\tau)F(\tau)\exp\left(\int_\tau^t K(s)\,\mathrm{d}s\right)\mathrm{d}\tau.$$

From [22] we have the following definition which characterizes viscoelastic solids (see also [46], Def. 6).

Definition 2.6 (Viscoelastic solid)**.** We say that a function $\phi \in L^1(\mathcal{J}; [0, \infty))$ characterize a viscoelastic solid if

$$0 \leq \left(1 - \int_0^t \phi(\tau)\,\mathrm{d}\tau\right)^{-1} < +\infty.$$

Observe that, since ϕ is non-negative a.e. in $\mathcal{J}$, we also have $\|\phi\|_{L^1(0,t)} \leq 1$.

Let us define the semi-norm $|v|_a^2 := a(v, v)$, which implies that

$$|v|_a^2 \lesssim \|v\|_{\mathcal{V}}^2, \tag{2.1}$$

due to the continuity of $a(\cdot, \cdot)$. Also, from Lemma 4.2.1 of [8] we have

$$a(u, v) \lesssim |u|_a\,|v|_a, \qquad \|\mathbb{A}u\|_{\mathcal{V}'}^2 \lesssim |u|_a^2. \tag{2.2}$$

We are now in position to prove the main result of this section.

Theorem 2.7. *Assume that $\mathbb{B}$ is surjective and that Assumption 2.1 holds. Also assume $a(\cdot,\cdot)$ is strongly coercive in $\mathcal{K}$, i.e., there exists α_0 such that*

$$a(v_0, v_0) \geq \alpha_0 \|v_0\|_{\mathcal{V}}^2 \qquad \forall v_0 \in \mathcal{K}.$$

If ϕ_a and ϕ_b characterize a viscoelastic solid, then, for every $f \in L^\ell(\mathcal{J};\mathcal{V}')$ and for every $g \in L^\ell(\mathcal{J};\mathcal{Q}')$, there exists a unique solution of Problem 1.1. Moreover, it follows that

$$\|u\|_{L^\ell(0,t;\mathcal{V})} + \|p\|_{L^\ell(0,t;\mathcal{Q})} \lesssim (1+\lambda)\|f\|_{L^\ell(0,t;\mathcal{V}')} + \frac{2+\lambda}{1+\lambda}\|g\|_{L^\ell(0,t;\mathcal{Q}')},$$

where the hidden constant is independent of λ.

Proof. We divide the the proof in two cases, and then sum the estimates by linearity. The first case corresponds when $(u,p) \in L^\ell(\mathcal{J};\mathcal{V}\times\mathcal{Q})$ solves

$$\begin{cases} \quad a(u,v) + b(v,p) = \langle f, v\rangle_{\mathcal{V}} + \displaystyle\int_0^t \Big[\widetilde{a}(t,s;(u(s),v)) + \widetilde{b}(t,s;(v,p(s)))\Big]\,\mathrm{d}s, \\ b(u,q) - \lambda(p,q)_{\mathcal{Q}} = 0, \end{cases} \tag{2.3}$$

for all $(v,q) \in \mathcal{V}\times\mathcal{Q}$, or equivalently in its operator form,

$$\begin{cases} \quad \mathbb{A}u + \mathbb{B}^*p = f + \displaystyle\int_0^t \Big[\widetilde{\mathbb{A}}(t,s)u(s) + \widetilde{\mathbb{B}}^*(t,s)p(s)\Big]\,\mathrm{d}s, \\ \mathbb{B}u - \lambda\mathfrak{R}_{\mathcal{Q}}p = 0, \end{cases} \tag{2.4}$$

a.e. in $\mathcal{J}$. We set $\widetilde{u} := \mathbb{L}_{\mathbb{B}}\lambda\mathfrak{R}_{\mathcal{Q}}p$, where $\mathbb{L}_{\mathbb{B}}$ is a lifting operator. The existence of this operator is guaranteed by Theorem 4.1.5 and Corollary 4.1.1 of [8]. Hence, we have that $\mathbb{B}u = \mathbb{B}\widetilde{u} = \lambda\mathfrak{R}_{\mathcal{Q}}p$. Defining $u_0 := u - \widetilde{u}$, we have that $u_0 \in \mathcal{K}$. Now we set $v = \widetilde{u}(t)$ in the first equation of (2.3) and since $p = \mathfrak{R}_{\mathcal{Q}}^{-1}\lambda^{-1}\mathbb{B}u$ we have

$$a(u,\widetilde{u}) + b\big(\widetilde{u}, \mathfrak{R}_{\mathcal{Q}}^{-1}\lambda^{-1}\mathbb{B}u\big) = \langle f, \widetilde{u}\rangle_{\mathcal{V}} + \int_0^t \Big[\widetilde{a}(t,s;(u(s),\widetilde{u}(t))) + \widetilde{b}\big(t,s;\big(\widetilde{u}(t), \mathfrak{R}_{\mathcal{Q}}^{-1}\lambda^{-1}\mathbb{B}u(s)\big)\big)\Big]\,\mathrm{d}s.$$

Using the fact that $\mathbb{B}\widetilde{u} = \mathbb{B}u$, from the equation above and Assumption 2.1-(ii) it follows that

$$\lambda^{-1}\|\mathbb{B}u\|_{\mathcal{Q}'}^2 = \langle f, \widetilde{u}\rangle_{\mathcal{V}} - a(u,\widetilde{u}) + \int_0^t \Big[\widetilde{a}(t,s;(u(s),\widetilde{u}(t))) + \phi_b(t-s)\lambda^{-1}\big\langle \mathbb{B}u(s), \mathfrak{R}_{\mathcal{Q}}^{-1}\mathbb{B}u(t)\big\rangle_{\mathcal{Q}}\Big]\,\mathrm{d}s. \tag{2.5}$$

Now we estimate $-a(u,\widetilde{u})$. To do this task, first we observe that (2.1), (2.2), and the splitting $u = \widetilde{u} + u_0$, yields to

$$-a(u,\widetilde{u}) = -a(\widetilde{u}+u_0,\widetilde{u}) = -a(\widetilde{u},\widetilde{u}) - a(u_0,\widetilde{u}) \lesssim -|\widetilde{u}|_a^2 + |\widetilde{u}|_a|u_0|_a. \tag{2.6}$$

On the other hand, testing the first equation in (2.3) with $v = u_0(t)$ gives

$$a(u,u_0) = \langle f, u_0\rangle_{\mathcal{V}} + \int_0^t \widetilde{a}(t,s;(u(s),u_0))\,\mathrm{d}s,$$

and then, from (2.1) and (2.2) we have that

$$\begin{aligned} |u_0|_a^2 = a(u_0,u_0) = a(u,u_0) - a(\widetilde{u},u_0) \\ &\lesssim \|f\|_{\mathcal{V}'}\|u_0\|_{\mathcal{V}} + |\widetilde{u}|_a|u_0|_a + (\phi_a * |u|_a)(t)\,|u_0|_a, \\ &\lesssim \|f\|_{\mathcal{V}'}|u_0|_a + |\widetilde{u}|_a|u_0|_a + (\phi_a * |u|_a)(t)\,|u_0|_a, \end{aligned} \tag{2.7}$$

where we have used the definition of $|\cdot|_a$. Then, (2.7) is reduced to

$$|u_0|_a \lesssim \|f\|_{\mathcal{V}'} + |\widetilde{u}|_a + (\phi_a * |u|_a)(t). \tag{2.8}$$

Inserting (2.8) in (2.6) yields to

$$-a(u,\widetilde{u}) \lesssim \|f\|_{\mathcal{V}'}|\widetilde{u}|_a + (\phi_a * |u|_a)(t)\,|\widetilde{u}|_a,$$

and replacing this inequality in (2.5) we obtain

$$\lambda^{-1}\|\mathbb{B}u\|_{\mathcal{Q}'} \lesssim \|f\|_{\mathcal{V}'} + (\phi_a * \|u_0\|_{\mathcal{V}})(t) + \big(\phi_a * \lambda^{-1}\|\mathbb{B}u\|_{\mathcal{Q}'}\big)(t) + \big(\phi_b * \lambda^{-1}\|\mathbb{B}u\|_{\mathcal{Q}'}\big)(t), \tag{2.9}$$

where we have used the inf-sup condition of $\mathbb{B}$ and the splitting $u = \tilde{u} + u_0$.

Now we will estimate $(\phi_a * \|u_0\|_{\mathcal{V}})(t)$. Invoking the $\mathcal{K}$-ellipticity of $a(\cdot,\cdot)$ in (2.8), along with (2.1), and the split $u = \widetilde{u} + u_0$ we obtain

$$\|u_0\|_{\mathcal{V}} \lesssim \|f\|_{\mathcal{V}'} + \|\widetilde{u}\|_{\mathcal{V}} + (\phi_a * \|\widetilde{u}\|_{\mathcal{V}})(t) + (\phi_a * \|u_0\|_{\mathcal{V}})(t).$$

From Gronwall's lemma we have that

$$\|u_0\|_{\mathcal{V}} \lesssim \widetilde{m}(t) + \int_0^t \chi(s)\widetilde{m}(s)\exp\bigg(\int_s^t \chi(\tau)\,\mathrm{d}\tau\bigg)\,\mathrm{d}s, \tag{2.10}$$

where

$$\widetilde{m}(t) := \|f\|_{\mathcal{V}'} + \|\widetilde{u}\|_{\mathcal{V}} + (\phi_a * \|\widetilde{u}\|_{\mathcal{V}})(t),$$

and

$$\chi(s) = \phi_a(t-s).$$

Since $\|\phi_a\|_{L^1(0,t)} \leq 1$ and ϕ_a is non-negative a.e. in $\mathcal{J}$, we obtain

$$\exp\bigg(\int_s^t \chi(\tau)\,\mathrm{d}\tau\bigg) = \exp\bigg(\int_s^t \phi_a(t-\tau)\,\mathrm{d}\tau\bigg) \lesssim \exp\bigg(\int_0^t \phi_a(t-\tau)\,\mathrm{d}\tau\bigg) < +\infty.$$

Hence, it follows that

$$\int_0^t \chi(s)\widetilde{m}(s)\exp\bigg(\int_s^t \chi(\tau)\,\mathrm{d}\tau\bigg)\,\mathrm{d}s \lesssim (\phi_a * \widetilde{m})(t).$$

On the other hand, observe that

$$(\phi_a * \widetilde{m})(t) = (\phi_a * \|f\|_{\mathcal{V}'})(t) + (\phi_a * \|\widetilde{u}\|_{\mathcal{V}})(t) + (\phi_a * (\phi_a * \|\widetilde{u}\|_{\mathcal{V}}))(t).$$

Since $\phi_a \in L^1(\mathcal{J};[0,\infty))$, from Fubini's Theorem and Lemma 2.4 we have that $(\phi_a * \phi_a)(t) \leq \|\phi_a\|^2_{L^1(0,t)}$. Hence we obtain

$$(\phi_a * \widetilde{m})(t) \lesssim (\phi_a * \|f\|_{\mathcal{V}'})(t) + (\phi_a * \|\widetilde{u}\|_{\mathcal{V}})(t) + \int_0^t \|\widetilde{u}(s)\|_{\mathcal{V}}\,\mathrm{d}s.$$

Then, from (2.10) we obtain that

$$\|u_0\|_{\mathcal{V}} \lesssim \widetilde{m}(t) + (\phi_a * \|f\|_{\mathcal{V}'})(t) + (\phi_a * \|\widetilde{u}\|_{\mathcal{V}})(t) + \int_0^t \|\widetilde{u}(s)\|_{\mathcal{V}}\,\mathrm{d}s. \tag{2.11}$$

Taking the convolution with ϕ_a in (2.11) and using the inf-sup condition of $\mathbb{B}$ together with the boundedness of ϕ_a, yields to

$$(\phi_a * \|u_0\|_{\mathcal{V}}) \lesssim (\phi_a * \|f\|_{\mathcal{V}'})(t) + (\phi_a * \|\mathbb{B}u\|_{\mathcal{Q}'})(t) + \int_0^t \|[f(s)\|_{\mathcal{V}'} + \|\mathbb{B}u(s)\|_{\mathcal{Q}'}]\,\mathrm{d}s. \tag{2.12}$$

Inserting this inequality in (2.9) gives

$$\lambda^{-1}\|\mathbb{B}u\|_{\mathcal{Q}'} \lesssim \|f\|_{\mathcal{V}'} + ([1+\phi_a] * \|f\|_{\mathcal{V}'})(t) + \big([1+\phi_a+\phi_b] * \lambda^{-1}\|\mathbb{B}u\|_{\mathcal{Q}'}\big)(t).$$

Hence, observing that ϕ_b also characterizes a viscoelastic solid, we use the boundedness of the kernel $(1 + \phi_a + \phi_b)$ and apply Gronwall's inequality in order to obtain

$$\lambda^{-1}\|\mathbb{B}u\|_{\mathcal{Q}'} \lesssim \|f\|_{\mathcal{V}'} + ([1+\phi_a] * \|f\|_{\mathcal{V}'})(t) + \int_0^t [\|f(s)\|_{\mathcal{V}'} + ([1+\phi_a] * \|f\|_{\mathcal{V}'})(s)]\,\mathrm{d}s. \tag{2.13}$$

From the fact that $\|\widetilde{u}\|_{\mathcal{V}} \lesssim \|\mathbb{B}u\|_{\mathcal{Q}'}$, we take the $L^\ell(0,t)$ norm in (2.13) and apply Lemma 2.4 to obtain the following estimate for $\widetilde{u}$

$$\|\widetilde{u}\|_{L^\ell(0,t;\mathcal{V})} \lesssim \lambda\|f\|_{L^\ell(0,t;\mathcal{V}')}. \tag{2.14}$$

To estimate u_0, we take the $L^\ell(0,t)$ norm in (2.11) and use Lemma 2.4 to obtain

$$\|u_0\|_{L^\ell(0,t;\mathcal{V})} \lesssim (1+\lambda)\|f\|_{L^\ell(0,t;\mathcal{V}')}. \tag{2.15}$$

The estimate for u follows directly from the triangle inequality

$$\|u\|_{L^\ell(0,t;\mathcal{V})} \lesssim (1+2\lambda)\|f\|_{L^\ell(0,t;\mathcal{V}')}. \tag{2.16}$$

On the other hand, from the second equation in (2.4) together with (2.13) and Lemma 2.4, we derive the following estimate for p,

$$\|p\|_{L^\ell(0,t;\mathcal{Q})} = \lambda^{-1}\|\mathbb{B}u\|_{L^\ell(0,t;\mathcal{Q}')} \lesssim \|f\|_{L^\ell(0,t;\mathcal{V}')}.$$

For the second part of the proof, we assume that u, p and g are such that the following system is satisfied

$$\begin{cases} a(u,v) + b(v,p) = \displaystyle\int_0^t \Big[\widetilde{a}(t,s;(u(s),v)) + \widetilde{b}(t,s;(v,p(s)))\Big]\,\mathrm{d}s, \\ b(u,q) - \lambda(p,q)_{\mathcal{Q}} = \langle g, q\rangle_{\mathcal{Q}}, \end{cases}$$

for all $(v,q) \in \mathcal{V}\times\mathcal{Q}$. Note that in operator form, problem above reads, a.e in $\mathcal{J}$, as follows

$$\begin{cases} \mathbb{A}u + \mathbb{B}^*p = \displaystyle\int_0^t \Big[\widetilde{\mathbb{A}}(t,s)u(s) + \widetilde{\mathbb{B}}^*(t,s)p(s)\Big]\,\mathrm{d}s, \\ \mathbb{B}u - \lambda\mathfrak{R}_{\mathcal{Q}}p = g. \end{cases} \tag{2.17}$$

Since $f = 0$, we take norms in the first equation of Problem 2.2 and use the boundedness of the linear operators and the Volterra kernels, in order to obtain

$$\|\mathbb{A}u + \mathbb{B}^*p\|_{\mathcal{V}'} \lesssim \int_0^t \|\mathbb{A}u(s) + \mathbb{B}^*p(s)\|_{\mathcal{V}'}\,\mathrm{d}s.$$

Then, from Gronwall's lemma we obtain that $\mathbb{A}u + \mathbb{B}^*p = 0$, or equivalently,

$$a(u,v) + b(v,p) = 0, \qquad \forall v \in \mathcal{V}.$$

Hence, we resort to Theorem 4.3.2 of [8] in order to obtain the remaining bounds:

$$\|u\|_{L^\ell(0,t;\mathcal{V})} \lesssim \|g\|_{L^\ell(0,t;\mathcal{Q}')} \quad \text{and} \quad \|p\|_{L^\ell(0,t;\mathcal{Q})} \lesssim \frac{1}{1+\lambda}\|g\|_{L^\ell(0,t;\mathcal{Q}')}.$$

Finally, by gathering the estimates for u and p with respect to f and g, gives the desired estimate. This concludes the proof. □

Since $0 < \lambda \leq \lambda_{\max}$, we observe that the stability constant is uniform with respect to the perturbation parameter in the sense that for all $\lambda > 0$, Theorem 2.7 guarantee that there exists a constant $C_\lambda > 0$, given by

$$C_\lambda := C[1 + \mathcal{O}(\lambda)] \leq C[1 + \mathcal{O}(\lambda_{\max})] < \infty,$$

where C is independent of λ, such that

$$\|u\|_{L^\ell(0,t;\mathcal{V})} + \|p\|_{L^\ell(0,t;\mathcal{Q})} \lesssim C_\lambda\big(\|f\|_{L^\ell(0,t;\mathcal{V}')} + \|g\|_{L^\ell(0,t;\mathcal{Q}')}\big). \tag{2.18}$$

Hereafter, for the sake of clarity, we will refer to the bound (2.18) in the applications of Theorem 2.7.

On the other hand, note that a bound like (2.18) is typically found in non-viscoelastic mixed formulations. This is an important fact, since in real applications, like the analysis of numerical methods for slender structures such as Timoshenko beams, Reissner–Mindlin plates, among others, the thickness parameter is the one that leads to the so called locking phenomenon. Now, when these structures admit viscoelastic properties, these results hold as well. For this reason, if λ represents the thickness parameter of some particular structure, Theorem 2.7 states that all the constants will not degenerate in our mixed viscoleastic formulation.

3. Semi-discrete problem

In this section we are interested in a discretization by conforming finite element spaces for Problem 1.1. With this goal in mind, and under suitable assumptions on discrete spaces, we adapt the classic theory for mixed formulations for our viscoelastic approach.

3.1. Semi-discrete abstract analysis

The goal of the present section is to analyze the semi-discrete counterpart of the proposed mixed problems and obtain *a priori* error estimates. Here, we consider the necessary hypotheses for the existence and uniqueness of semi-discrete solutions such as ellipticity in the kernel and the discrete inf-sup condition (see for instance [2, 45] for further details related to the existence of semi-discrete solutions of Volterra equations of the second kind).

Hence, this section will be focused on the derivation of error estimates which are characterized by having constants that do not deteriorate when the parameter λ is small.

Let us introduce the following assumption.

Assumption 3.1. *Assume that there exist two finite dimensional spaces $\mathcal{V}_h$ and $\mathcal{Q}_h$ such that $\mathcal{V}_h \subset \mathcal{V}$ and $\mathcal{Q}_h \subset \mathcal{Q}$. Together with the continuous space kernel $\mathcal{K}$ we consider its discrete counterpart*

$$\mathcal{K}_h := \{v_h \in \mathcal{V}_h : b(v_h, q_h) = 0, \qquad \forall q_h \in \mathcal{Q}_h\},$$

such that there exist constants α_d, β_d, both positive and independent of h and λ, such that

$$a\big(v_h^0, v_h^0\big) \geq \alpha_d \|v_h^0\|_{\mathcal{V}}^2 \quad \forall v_h^0 \in \mathcal{K}_h, \qquad \sup_{v\in\mathcal{V}_h} \frac{b(v_h, q_h)}{\|v_h\|_{\mathcal{V}}} \geq \beta_d \|q_h\|_{\mathcal{Q}}, \quad \forall q_h \in \mathcal{Q}_h.$$

Throughout this section, families of conforming finite elements are considered.

For simplicity, we define the corresponding errors as follows

$$\mathsf{e}_u := u_h - u = \vartheta_u - \eta_u, \qquad \mathsf{e}_p := p_h - p = \vartheta_p - \eta_p,$$

where $\vartheta_u := u_h - u_I$, $\vartheta_p := p_h - p_I$, $\eta_u = u - u_I$, and $\eta_p = p - p_I$. Here, $u_I \in \mathcal{V}_h$ and $p_I \in \mathcal{Q}_h$ represent general interpolations of u and p, respectively (see for instace [8], Chap. 5 or [39], Chap. 4).

In what follows we analyze the semi-discretization of the perturbed mixed formulation analyzed in the previous section. The following problem corresponds to the semi-discretized version of Problem 1.1.

Problem 3.2. Find $(u_h, p_h) \in L^\ell(\mathcal{J}; \mathcal{V}_h \times \mathcal{Q}_h)$ such that

$$\begin{cases} a(u_h, v_h) + b(v_h, p_h) = \langle f, v_h\rangle_{\mathcal{V}} + \displaystyle\int_0^t \Big[\widetilde{a}(t, s; (u_h(s), v_h)) + \widetilde{b}(t, s; (v_h, p_h(s)))\Big]\, \mathrm{d}s, \\ b(u_h, q_h) - \lambda(p_h, q_h)_{\mathcal{Q}} = \langle g, q_h\rangle_{\mathcal{Q}}, \end{cases}$$

for all $(v_h, q_h) \in \mathcal{V}_h \times \mathcal{Q}_h$.

The existence and uniqueness, as well as the discrete stability estimate of the semi-discrete solution, follows from Assumption 3.1 and Theorem 2.7. Hence, we obtain the following system, from subtracting Problem 1.1 and Problem 3.2:

$$\begin{cases} a(\mathsf{e}_u, v_h) + b(v_h, \mathsf{e}_p) = \displaystyle\int_0^t \Big[\widetilde{a}(t, s; (\mathsf{e}_u(s), v_h)) + \widetilde{b}(t, s; (v_h, \mathsf{e}_p(s)))\Big]\, \mathrm{d}s, \\ b(\mathsf{e}_u, q_h) - \lambda(\mathsf{e}_p, q_h)_{\mathcal{Q}} = 0, \end{cases} \tag{3.1}$$

for all $(v_h, q_h) \in \mathcal{V}_h \times \mathcal{Q}_h$. Then, from the linearity of $a(\cdot,\cdot)$, $b(\cdot,\cdot)$ and the history bilinear forms, we rewrite the problem above as follows: Find $(\vartheta_u, \vartheta_p) \in L^\ell(\mathcal{J}; \mathcal{V}_h \times \mathcal{Q}_h)$ such that

$$\begin{cases} a(\vartheta_u, v_h) + b(v_h, \vartheta_p) = \langle \mathcal{F}, v_h\rangle_{\mathcal{V}} + \displaystyle\int_0^t \Big[\widetilde{a}(t, s; (\vartheta_u(s), v_h)) + \widetilde{b}(t, s; (v_h, \vartheta_p(s)))\Big]\, \mathrm{d}s, \\ b(\vartheta_u, q_h) - \lambda(\vartheta_p, q_h)_{\mathcal{Q}} = \langle \mathcal{G}, q_h\rangle_{\mathcal{Q}}, \end{cases} \tag{3.2}$$

for all $(v_h, q_h) \in \mathcal{V}_h \times \mathcal{Q}_h$, where

$$\langle \mathcal{F}, v_h\rangle_{\mathcal{V}} = a(\eta_u, v_h) + b(v_h, \eta_p) - \int_0^t \Big[\widetilde{a}(t, s; (\eta_u(s), v_h) + \widetilde{b}(t, s; (v_h, \eta_p(s)))\Big]\, \mathrm{d}s, \tag{3.3}$$

$$\langle \mathcal{G}, q_h\rangle_{\mathcal{Q}} = b(\eta_u, q_h) - \lambda(\eta_p, q_h)_{\mathcal{Q}}. \tag{3.4}$$

Then, from Theorem 2.7 we have the following result.

Theorem 3.3. *Together with Assumption 3.1, assume that (u, p) is the unique solution of Problem 1.1 and let (u_h, p_h) be the unique solution of Problem 3.2. Then, the estimate*

$$\|u_h - u\|_{L^\ell(0,t;\mathcal{V})} + \|p_h - p\|_{L^\ell(0,t;\mathcal{Q})} \lesssim \inf_{v_h\in\mathcal{V}_h} \|u - v_h\|_{L^\ell(0,t;\mathcal{V})} + \inf_{q_h\in\mathcal{Q}_h} \|p - q_h\|_{L^\ell(0,t;\mathcal{Q})},$$

holds, where the hidden constant is uniform with respect to λ.

Proof. Let $u_I \in L^\ell(\mathcal{J}; \mathcal{V}_h)$ and $p_I \in L^\ell(\mathcal{J}; \mathcal{Q}_h)$. Then, applying Theorem 2.7 in (3.2), we have

$$\|\vartheta_u\|_{L^\ell(0,t;\mathcal{V})} + \|\vartheta_p\|_{L^\ell(0,t;\mathcal{Q})} \lesssim \|\mathcal{F}\|_{L^\ell(0,t;\mathcal{V}')} + \|\mathcal{G}\|_{L^\ell(0,t;\mathcal{Q}')}.$$

On the other hand, estimating (3.3) and (3.4) gives

$$\begin{aligned} \|\mathcal{F}\|_{L^\ell(0,t;\mathcal{V}')} &\lesssim \|u - u_I\|_{L^\ell(0,t;\mathcal{V})} + \|p - p_I\|_{L^\ell(0,t;\mathcal{Q})}, \\ \|\mathcal{G}\|_{L^\ell(0,t;\mathcal{Q}')} &\lesssim \|u - u_I\|_{L^\ell(0,t;\mathcal{V})} + \lambda\|p - p_I\|_{L^\ell(0,t;\mathcal{Q})}, \end{aligned}$$

hence, from the triangle inequality we obtain

$$\begin{aligned} \|\mathsf{e}_u\|_{L^\ell(0,t;\mathcal{V})} \le \|\vartheta_u - \eta_u\|_{L^\ell(0,t;\mathcal{V})} &\le \|\vartheta_u\|_{L^\ell(0,t;\mathcal{V})} + \|\eta_u\|_{L^\ell(0,t;\mathcal{V})} \\ &\lesssim \big[\|\eta_u\|_{L^\ell(0,t;\mathcal{V})} + \|\eta_p\|_{L^\ell(0,t;\mathcal{Q})}\big]. \end{aligned}$$

Similarly, we have

$$\begin{aligned} \|\mathsf{e}_p\|_{L^\ell(0,t;\mathcal{Q})} \le \|\vartheta_p - \eta_p\|_{L^\ell(0,t;\mathcal{Q})} &\le \|\vartheta_p\|_{L^\ell(0,t;\mathcal{Q})} + \|\eta_p\|_{L^\ell(0,t;\mathcal{Q})} \\ &\lesssim \|\eta_u\|_{L^\ell(0,t;\mathcal{V})} + \|\eta_p\|_{L^\ell(0,t;\mathcal{Q})}. \end{aligned}$$

We conclude the proof by taking the infimum over all u_I and p_I. ◻

3.2. Error estimates in weaker norms

For the sake of completeness, in this section we include some additional estimates using a duality argument in the sense of the Volterra theory (see [46] for instance). It is important to remark that all the forthcoming results are a adaptation of the standard arguments in elliptic problems, such as the Aubin–Nitsche trick. The arguments provided here will be useful for the viscoelastic Timoshenko beam model (see Sect. 4).

Let us consider two spaces $\mathcal{V}_-$ and $\mathcal{Q}_-$, where the "$_-$" index indicates a less regular spaces than $\mathcal{V}$ and $\mathcal{Q}$, respectively, satisfying the following dense inclusions

$$\mathcal{V} \hookrightarrow \mathcal{V}_- \quad \text{and} \quad \mathcal{Q} \hookrightarrow \mathcal{Q}_-. \tag{3.5}$$

Our aim is to estimate $\|u-u_h\|_{L^\ell(0,t;\mathcal{V}_-)}$ and $\|p-p_h\|_{L^\ell(0,t;\mathcal{Q}_-)}$. To accomplish this task, we define

$$\mathcal{V}_+' := (\mathcal{V}_-)', \quad \mathcal{Q}_+' := (\mathcal{Q}_-)'.$$

The "+" suggest that we have more regular dual spaces. On the other hand, the inclusions provided in (3.5) imply

$$\mathcal{V}_+' \hookrightarrow \mathcal{V}', \quad \mathcal{Q}_+' \hookrightarrow \mathcal{Q}'.$$

Let $\mathcal{V}_{++}$ and $\mathcal{Q}_{++}$ be two spaces, where the double subindex "++" denotes more regular spaces that $\mathcal{V}$ and $\mathcal{Q}$, respectively, satisfying the inclusions

$$\mathcal{V}_{++} \hookrightarrow \mathcal{V}, \quad \mathcal{Q}_{++} \hookrightarrow \mathcal{Q}.$$

Now we introduce a dual-backward mixed formulation of Problem 1.1. To do this task, let r denote the Hölder conjugate index of ℓ. Then, for any $\tau \in \mathcal{J}$ and for any $(f_+, g_+) \in L^r(0,\tau;\mathcal{V}_+' \times \mathcal{Q}_+')$, we consider the dual problem: find $(w,m) \in L^r(0,\tau;\mathcal{V}\times\mathcal{Q})$ such that a.e. in $[0,\tau]$,

$$\begin{cases} a(v,w) + b(v,m) = \langle f_+, v\rangle_{\mathcal{V}_+'\times\mathcal{V}} + \displaystyle\int_t^\tau \Big[\widetilde{a}(s,t;v,w(s)) + \widetilde{b}(s,t;v,m(s))\Big]\,\mathrm{d}s, \\ b(w,q) - \lambda(q,m)_{\mathcal{Q}} = \langle g_+, q\rangle_{\mathcal{Q}_+'\times\mathcal{Q}}, \end{cases} \tag{3.6}$$

for all $(v,q) \in \mathcal{V}\times\mathcal{Q}$.

Setting $\xi := \tau - t$, $\eta = \tau - s$ and defining

$$\begin{aligned} &\overline{w}(\cdot) := w(\tau - \cdot), \quad \overline{m}(\cdot) := m(\tau-\cdot), \quad \overline{f}_+(\xi) := f_+(\tau-\xi), \quad \overline{g}_+(\xi) := g_+(\tau-\xi), \\ &\overline{a}(\xi,\eta,(\cdot,v)) := \widetilde{a}(\tau-\eta,\tau-\xi,(v,\cdot)), \qquad \overline{b}(\xi,\eta,(v,\cdot)) := \widetilde{b}(\tau-\eta,\tau-\xi,(v,\cdot)), \end{aligned}$$

it follows that the backward problem can be written in forward form as: Find $(w,m) \in L^r(0,\tau;\mathcal{V}\times\mathcal{Q})$, such that for a.e. $\xi\in[0,\tau]$,

$$\begin{cases} a(\overline{w},v) + b(v,\overline{m}) = \langle \overline{f}_+, v\rangle_{\mathcal{V}_+'\times\mathcal{V}} + \displaystyle\int_0^\xi \big[\overline{a}(\xi,\eta;(\overline{w}(\eta),v)) + \overline{b}(\xi,\eta;v,\overline{m}(\eta))\big]d\eta, \\ b(\overline{w},q) - \lambda(\overline{m},q)_{\mathcal{Q}} = \langle \overline{g}_+, q\rangle_{\mathcal{Q}_+'\times\mathcal{Q}}, \end{cases} \tag{3.7}$$

for all $(v,q)\in\mathcal{V}\times\mathcal{Q}$. Now, this is basically the same as Problem 1.1. Hence, in order to apply all the previous stability and semi-discrete results to this dual problem, we have to guarantee that Assumption 2.1 is satisfied. Assumption 2.1-(i) is straightforward. Assumption 2.1-(iii) is satisfied because $\|\overline{f}_+\|_{\mathcal{V}_+'}, \|\overline{g}_+\|_{\mathcal{Q}_+'} \in L^r(0,\tau)$. For Assumption 2.1-(ii) we observe that

$$|\overline{a}(\xi,\eta;(\overline{w}(\eta),v))| \lesssim \phi_a((\tau-\eta)-(\tau-\xi))\|\overline{w}\|_{\mathcal{V}}\|v\|_{\mathcal{V}} \lesssim \phi_a(\xi-\eta)\|\overline{w}\|_{\mathcal{V}}\|v\|_{\mathcal{V}}.$$

Similarly, $|\overline{b}(\xi,\eta;v,\overline{\psi}(\eta))| \lesssim \phi_b(\xi-\eta)\|v\|_{\mathcal{V}}\|\overline{\psi}\|_{\mathcal{Q}}$. Then, Theorem 2.7 guarantees that

$$\|w\|_{L^r(0,\tau;\mathcal{V})} + \|m\|_{L^r(0,\tau;\mathcal{Q})} \lesssim \|f_+\|_{L^r(0,\tau;\mathcal{V}_+')} + \|g_+\|_{L^r(0,\tau;\mathcal{Q}_+')}.$$

In order to simplify the presentation of the material, we define the errors $\mathsf{e}_w := w_h - w$ and $\mathsf{e}_m := m_h - m$, where the dependence on time is omitted if no confusion arises.

Now we are in position to establish our weak norm estimate.

Theorem 3.4. *Under the hypotheses of Theorem 3.3, assume that the solution to the dual problem (3.6) belongs to $L^r(0,\tau;\mathcal{V}_{++}\times\mathcal{Q}_{++})$ a.e. in $[0,\tau]$ and the estimate*

$$\|w\|_{L^r(0,\tau;\mathcal{V}_{++})}+\|m\|_{L^r(0,\tau;\mathcal{Q}_{++})}\lesssim \|f_+\|_{L^r\left(0,\tau;\mathcal{V}_+'\right)}+\|g_+\|_{L^r\left(0,\tau;\mathcal{Q}_+'\right)},$$

holds with the hidden constant is independent of f_+ and g_+. Then, we have

$$\|u-u_h\|_{L^\ell(0,t;\mathcal{V}_-)}+\|p-p_h\|_{L^\ell(0,t;\mathcal{Q}_-)}\lesssim\left(\inf_{v\in\mathcal{V}_h}\|u-v\|_{L^\ell(0,t;\mathcal{V})}+\inf_{q\in\mathcal{Q}_h}\|p-q\|_{L^\ell(0,t;\mathcal{Q})}\right)(l(h)+n(h)),$$

where

$$l(h):=\sup_{w\in L^r(0,t;\mathcal{V}_{++})}\inf_{w_h\in L^r(0,\tau;\mathcal{V}_h)}\frac{\|w-w_h\|_{L^r(0,t;\mathcal{V})}}{\|w\|_{L^r(0,t;\mathcal{V}_{++})}},$$
$$n(h):=\sup_{m\in L^r(0,t;\mathcal{Q}_{++})}\inf_{m_h\in L^r(0,\tau;\mathcal{Q}_h)}\frac{\|m-m_h\|_{L^r(0,t;\mathcal{Q})}}{\|m\|_{L^r(0,t;\mathcal{Q}_{++})}},$$

and the hidden constant is independent of h and λ.

Proof. Taking time dependent test functions $v\in L^\ell(0,\tau;\mathcal{V})$ in the first equation of (3.6), integrating in $[0,\tau]$, and interchanging the order of integration gives,

$$\begin{aligned}\int_0^\tau \langle f_+,v(t)\rangle_{\mathcal{V}_+'\times\mathcal{V}}\,\mathrm{d}t\\ =\int_0^\tau\left\{a(v(t),w(t))+b(v(t),m(t))-\int_0^t\left[\widetilde{a}(t,s;(v(s),w(t)))+\widetilde{b}(t,s;(v(s),m(t)))\right]\mathrm{d}s\right\}\mathrm{d}t.\end{aligned}\tag{3.8}$$

On the other hand, taking $q\in L^\ell(0,\tau;\mathcal{V})$ in the second equation of (3.6) gives

$$\int_0^\tau\langle g_+,q(t)\rangle_{\mathcal{Q}_+'\times\mathcal{Q}}\,\mathrm{d}t=\int_0^\tau\left[b(w(t),q(t))-\lambda(q(t),m(t))_{\mathcal{Q}}\right]\mathrm{d}t.\tag{3.9}$$

Set $v=u-u_h$ in (3.8) and $q=p-p_h$ in (3.9) in order to obtain

$$\begin{aligned}\int_0^\tau \langle f_+,\mathsf{e}_u(t)\rangle_{\mathcal{V}_+'\times\mathcal{V}}\,\mathrm{d}t\\ =\int_0^\tau\left\{a(\mathsf{e}_u(t),w(t))+b(\mathsf{e}_u(t),m(t))-\int_0^t\left[\widetilde{a}(t,s;(\mathsf{e}_u(s),w(t)))+\widetilde{b}(t,s;(\mathsf{e}_u(s),m(t)))\right]\mathrm{d}s\right\}\mathrm{d}t,\end{aligned}\tag{3.10}$$

and

$$\int_0^\tau\langle g_+,\mathsf{e}_p(t)\rangle_{\mathcal{Q}_+'\times\mathcal{Q}}\,\mathrm{d}t=\int_0^\tau\left[b(w(t),\mathsf{e}_p(t))-\lambda(\mathsf{e}_p(t),m(t))_{\mathcal{Q}}\right]\mathrm{d}t.\tag{3.11}$$

For $z_1\in L^r(0,\tau)$ we set $f_+(t)=z_1(t)\mathsf{e}_u(t)\|\mathsf{e}_u(t)\|_{\mathcal{V}_-}^{-1}$. Then we obtain that $\langle f_+,\mathsf{e}_u\rangle_{\mathcal{V}_+'\times\mathcal{V}_-}=z_1(t)\|\mathsf{e}_u\|_{\mathcal{V}_-}$. This result applied on (3.10) yields to

$$\begin{aligned}\int_0^\tau z_1(t)\|\mathsf{e}_u(t)\|_{\mathcal{V}_-}\,\mathrm{d}t=\int_0^\tau&\left\{a(\mathsf{e}_u(t),w(t))+b(\mathsf{e}_u(t),m(t))\right.\\ &\left.-\int_0^t\left[\widetilde{a}(t,s;(\mathsf{e}_u(s),w(t)))+\widetilde{b}(t,s;(\mathsf{e}_u(s),m(t)))\right]\mathrm{d}s\right\}\mathrm{d}t.\end{aligned}$$

Similarly, for $z_2 \in L^r(0,\tau)$, if $g_+(t) = z_2(t)\mathsf{e}_p(t)\|\mathsf{e}_p(t)\|_{\mathcal{Q}_-}^{-1}$, then we proceed as before to obtain that $\langle g_+, \mathsf{e}_p\rangle_{\mathcal{Q}'_+\times\mathcal{Q}_-} = z_2(t)\|\mathsf{e}_p\|_{\mathcal{Q}_-}$. Replacing this in (3.11), yields to

$$\int_0^\tau z_2(t)\|\mathsf{e}_p(t)\|_{\mathcal{Q}_-}\,\mathrm{d}t = \int_0^\tau [b(w(t),\mathsf{e}_p(t)) - \lambda(\mathsf{e}_p(t), m(t))_{\mathcal{Q}}]\,\mathrm{d}t.$$

On the other hand from (3.1) we have that

$$\begin{cases} a(\mathsf{e}_u, w_h) + b(w_h, \mathsf{e}_p) = \displaystyle\int_0^t \Big[\widetilde{a}(t,s;(\mathsf{e}_u(s), w_h)) + \widetilde{b}(t,s;(w_h,\mathsf{e}_p(s)))\Big]\,\mathrm{d}s = 0,\\ b(\mathsf{e}_u, m_h) - \lambda(\mathsf{e}_p, m_h)_{\mathcal{Q}} = 0,\end{cases}$$

for all $w_h \in \mathcal{V}_h$ and for all $m_h \in \mathcal{Q}_h$. Hence, using the continuity of the bilinear forms, the viscoelasticity characterization of ϕ_a and ϕ_b, Hölder's inequality, and Lemma 2.4, we obtain

$$\begin{aligned}\int_0^\tau \big(z_1(t)\|\mathsf{e}_u\|_{\mathcal{V}_-} + z_2(t)\|\mathsf{e}_p\|_{\mathcal{Q}_-}\big)\,\mathrm{d}t &= \int_0^\tau \Big\{a(\mathsf{e}_u,\mathsf{e}_w) + b(\mathsf{e}_u,\mathsf{e}_m) + b(\mathsf{e}_w,\mathsf{e}_p)\\ &\quad - \lambda(\mathsf{e}_p,\mathsf{e}_m)_{\mathcal{Q}} - \int_0^t \Big[\widetilde{a}(t,s;(\mathsf{e}_u(s),\mathsf{e}_w)) + \widetilde{b}(t,s;(\mathsf{e}_u(s),\mathsf{e}_m))\Big]\,\mathrm{d}s\Big\}\,\mathrm{d}t\\ &\lesssim \big(\|\mathsf{e}_u\|_{L^\ell(0,\tau;\mathcal{V})} + \|\mathsf{e}_p\|_{L^\ell(0,\tau;\mathcal{Q})}\big)\big(\|\mathsf{e}_w\|_{L^r(0,\tau;\mathcal{V})} + \|\mathsf{e}_m\|_{L^r(0,\tau;\mathcal{Q})}\big).\end{aligned} \tag{3.12}$$

On the other hand, we have that

$$\|\mathsf{e}_u\|_{L^\ell(0,\tau;\mathcal{V}_-)} = \sup_{z_1}\Big\{\Big|\int_0^\tau z_1(t)\|\mathsf{e}_u(t)\|_{\mathcal{V}_-}\,\mathrm{d}t\Big| : \|z_1\|_{L^r(0,\tau)} = 1\Big\},$$

and

$$\|\mathsf{e}_p\|_{L^\ell(0,\tau;\mathcal{Q}_-)} = \sup_{z_2}\Big\{\Big|\int_0^\tau z_2(t)\|\mathsf{e}_p(t)\|_{\mathcal{Q}_-}\,\mathrm{d}t\Big| : \|z_2\|_{L^r(0,\tau)} = 1\Big\},$$

for $\ell \in [1,\infty]$. Therefore, equation (3.12) becomes

$$\|\mathsf{e}_u\|_{L^\ell(0,\tau;\mathcal{V}_-)} + \|\mathsf{e}_p\|_{L^\ell(0,\tau;\mathcal{Q}_-)} \lesssim \big(\|\mathsf{e}_u\|_{L^\ell(0,\tau;\mathcal{V})} + \|\mathsf{e}_p\|_{L^\ell(0,\tau;\mathcal{Q})}\big)\big(\|\mathsf{e}_w\|_{L^r(0,\tau;\mathcal{V})} + \|\mathsf{e}_m\|_{L^r(0,\tau;\mathcal{Q})}\big). \tag{3.13}$$

Observe that from the definition of $l(h)$ and $n(h)$ we have

$$\begin{aligned}\inf_{w_h\in L^r(0,\tau;\mathcal{V}_h)} \|w - w_h\|_{L^r(0,\tau;\mathcal{V})} &\le l(h)\|w\|_{L^r(0,\tau;\mathcal{V}_{++})},\\ \inf_{m_h\in L^r(0,\tau;\mathcal{Q}_h)} \|m - m_h\|_{L^r(0,\tau;\mathcal{Q})} &\le n(h)\|m\|_{L^r(0,\tau;\mathcal{Q}_{++})}.\end{aligned}$$

Adding the two inequalities above we have

$$\inf_{w_h\in L^r(0,\tau;\mathcal{V}_h)} \|w - w_h\|_{L^r(0,\tau;\mathcal{V})} + \inf_{m_h\in L^r(0,\tau;\mathcal{Q}_h)} \|m - m_h\|_{L^r(0,\tau;\mathcal{Q})} \lesssim l(h) + n(h),$$

where we have used that $\|f_+\|_{L^r(0,\tau;\mathcal{V}'_+)} + \|g_+\|_{L^r(0,\tau;\mathcal{Q}'_+)} = 2$. Taking the infimum in (3.13) for w_h and m_h, in $\mathcal{V}_h$ and $\mathcal{Q}_h$, respectively, gives

$$\|\mathsf{e}_u\|_{L^\ell(0,\tau;\mathcal{V}_-)} + \|\mathsf{e}_p\|_{L^\ell(0,\tau;\mathcal{Q}_-)} \lesssim \big(\|\mathsf{e}_u\|_{L^\ell(0,\tau;\mathcal{V})} + \|\mathsf{e}_p\|_{L^\ell(0,\tau;\mathcal{Q})}\big)[l(h) + n(h)]. \tag{3.14}$$

Since τ is arbitrary, we conclude the proof taking $\tau = t$ and applying Theorem 3.3 to the semi-discrete error estimates for u and p in the right side of (3.14). □

4. Applications to linear viscoelastic slender structures

This section is devoted to the application of the proposed abstract framework in the formulation and analysis of numerical methods for viscoelastic structures. The study will focus on Timoshenko beams and Reissner–Mindlin plates. These are well-known elastic structures for which mixed formulations have been carried out in order to study the numerical locking. A usual constitutive equation for linear isotropic viscoelastic material is of the form:

$$\boldsymbol{\sigma}(t) = \boldsymbol{Q}(0)\boldsymbol{\varepsilon}(t) - \int_0^t \dot{\boldsymbol{Q}}(t-s)\boldsymbol{\varepsilon}(s)\,\mathrm{d}s,$$

where $\boldsymbol{Q}$ is the general fourth order viscoelastic tensor, $\dot{\boldsymbol{Q}}(t-s) = \mathrm{d}\boldsymbol{Q}(t-s)/\mathrm{d}t$, and $\boldsymbol{\varepsilon}(\cdot)$ is the Green–Lagrange strain tensor [5, 22, 34]. The present analysis considers bounded creep materials, which yields to

$$\begin{aligned}\sigma_{ij}(t) &= E(0)Q_{ijkl}\varepsilon_{kl}(t) - \int_0^t \dot{E}(t-s)Q_{ijkl}\varepsilon_{kl}(s)\,\mathrm{d}s\\ \sigma_{i3}(t) &= G(0)D_{i3k3}\varepsilon_{k3}(t) - \int_0^t \dot{G}(t-s)D_{i3k3}\varepsilon_{k3}(s)\,\mathrm{d}s, \qquad \sigma_{33}(t) = 0,\end{aligned} \tag{4.1}$$

where Q_{ijkl} and D_{ijkl} are unit elastic tensors that account for the shear, membrane, and bending contributions of the structure. The functions $E(t)$ and $G(t)$ correspond to the relaxation and shear modulus, respectively. The action of the unit elastic tensors on $\boldsymbol{\varepsilon}(\cdot)$ is given by

$$Q_{ijkl}\varepsilon_{kl}(t) := \frac{1}{(1-\nu^2)}[(1-\nu)\varepsilon_{ij}(t) + v\delta_{ij}\varepsilon_{kk}(t)], \qquad D_{i3k3}\varepsilon_{k3}(t) := \frac{k_s}{1+\nu}\varepsilon_{i3}(t),$$

where k_s is the correction factor, and ν is the Poisson ratio. Also, for bounded creep materials, the relaxation and shear modulus can be expressed in terms of a Prony series of order P as

$$E(t) = E_0 + \sum_{i=1}^{P} E_i e^{-t/\tau_i^E}, \qquad G(t) = G_0 + \sum_{i=1}^{P} G_i e^{-t/\tau_i^G},$$

where $E_0 = E(0), G_0 = G(0)$, and τ_i^E, τ_i^G are relaxation times. If we normalize the Prony series such that $E(0) = G(0) = 1$, then we observe that the constitutive relations (4.1) are reduced to

$$\begin{aligned}\sigma_{ij}(t) &= Q_{ijkl}\varepsilon_{kl}(t) - \int_0^t \dot{E}(t-s)Q_{ijkl}\varepsilon_{kl}(s)\,\mathrm{d}s,\\ \sigma_{i3}(t) &= D_{i3k3}\varepsilon_{k3}(t) - \int_0^t \dot{G}(t-s)D_{i3k3}\varepsilon_{k3}(s)\,\mathrm{d}s, \qquad \sigma_{33}(t) = 0.\end{aligned} \tag{4.2}$$

Hence, we choose $\phi_a(t) = -\dot{E}(t)$ and $\phi_b(t) = -\dot{G}(t)$. It is important to observe that this selection satisfies

$$\|\phi_a(t)\|_{L^1(0,t)} \leq 1, \qquad \|\phi_b(t)\|_{L^1(0,t)} \leq 1,$$

as is required in our analysis.

On the other hand, the natural relation between E and G given by $G(t) = E(t)/(2(1+\nu))$ is assumed (see, for instance [11]). Hence, the corresponding characterization functions satisfy $\phi_a(t) = 2(1+\nu)\phi_b(t)$. For other choices of ϕ, like in isotropic linear materials, we refer to Chapter 8 of [24].

In what follows, let $\Omega \subset \mathbb{R}^n$, $n \in \{1,2\}$, be an open and convex domain with boundary $\partial\Omega$. We denote by $L^2(\Omega)$ and $H^l(\Omega)$ the usual Lebesgue and Sobolev spaces, with the convention $H^0(\Omega) = L^2(\Omega)$. The spaces are endowed with standard norms $\|\cdot\|_{L^2(\Omega)}$ and $\|\cdot\|_{H^l(\Omega)}$. Let $H_0^1(\Omega)$ be the subspace of $H^1(\Omega)$ consisting of functions that vanish in $\partial\Omega$. For $n = 2$, we define by $\boldsymbol{L}^2(\Omega) := L^2(\Omega)^2$ the space of Lebesgue measure space of vector functions. We denote by $\boldsymbol{H}^l(\Omega)$ and $\boldsymbol{H}_0^1(\Omega)$ the vectorial version of $H^l(\Omega)$ and $H_0^1(\Omega)$, respectively.

We denote by DOF the number of degrees of freedom. To measure the errors for several values of ℓ in $L^\ell(\cdot\,;\,\cdot)$, we define

$$\mathtt{e}_{0,\ell}(f) := \frac{\|f - f_h\|_{L^\ell(\mathcal{J};L^2(\Omega))}}{\|f\|_{L^\ell(\mathcal{J};L^2(\Omega))}}, \quad \mathtt{e}_{\mathbf{0},\ell}(\boldsymbol{f}) := \frac{\|\boldsymbol{f} - \boldsymbol{f}_h\|_{L^\ell(\mathcal{J};\boldsymbol{L}^2(\Omega))}}{\|\boldsymbol{f}\|_{L^\ell(\mathcal{J};\boldsymbol{L}^2(\Omega))}},$$
$$\mathtt{e}_{1,\ell}(f) := \frac{\|f - f_h\|_{L^\ell(\mathcal{J};H^1(\Omega))}}{\|f\|_{L^\ell(\mathcal{J};H^1(\Omega))}}, \quad \mathtt{e}_{\mathbf{1},\ell}(\boldsymbol{f}) := \frac{\|\boldsymbol{f} - \boldsymbol{f}_h\|_{L^\ell(\mathcal{J};\boldsymbol{H}^1(\Omega))}}{\|\boldsymbol{f}\|_{L^\ell(\mathcal{J};\boldsymbol{H}^1(\Omega))}},$$

for every scalar function f and every vector function $\boldsymbol{f}$, respectively. Moreover, we define the experimental rates of convergence $\mathtt{r}_i(\cdot)$ and $\mathtt{r}_{\boldsymbol{i}}(\cdot)$ as

$$\mathtt{r}_{i,\ell}(\cdot) := \frac{\log\left(\mathtt{e}_{i,\ell}(\cdot)/\mathtt{e}'_{i,\ell}(\cdot)\right)}{\log(h/h')}, \qquad \mathtt{r}_{\boldsymbol{i},\ell}(\cdot) := \frac{\log\left(\mathtt{e}_{\boldsymbol{i},\ell}(\cdot)/\mathtt{e}'_{\boldsymbol{i},\ell}(\cdot)\right)}{\log(h/h')},$$

where $\mathtt{e}_{i,\ell}$ and $\mathtt{e}'_{i,\ell}$ (resp. $\mathtt{e}_{\boldsymbol{i},\ell}$ and $\mathtt{e}'_{\boldsymbol{i},\ell}$) denote two consecutive errors and h and h' their corresponding mesh sizes.

Now, we briefly discuss a fully discrete system coming from the introduction of (4.1) and (4.2) into the general semi-discrete system given in Problem 3.2. This approach takes advantage of (4.2) and the Prony series. Since we are dealing with normalized relaxation modulus and a conforming numerical scheme, we have the following representation of the resulting matrix system

$$\boldsymbol{K}\boldsymbol{\alpha}(t) - \int_0^t \widetilde{\boldsymbol{K}}(t-s)\boldsymbol{\alpha}(s)\,\mathrm{d}s = \boldsymbol{F}(t) \tag{4.3}$$

where $\boldsymbol{K}$, and $\boldsymbol{\alpha}$ are the stiffness matrix, and the solution vector, respectively, obtained by using specified finite elements spaces. The vector $\boldsymbol{F}$ stores the load contribution and $\widetilde{\boldsymbol{K}}$ stores the history of the deformations as a function of $\dot{E}$ and $\dot{G}$. Thanks to (4.2), for linear problems with prony series relaxation modulus, one can think of $\widetilde{\boldsymbol{K}}(t-s)$ as $\dot{E}(t-s)\boldsymbol{K}$. To obtain a fully discretization, we focus on the system (4.3). Start by choosing a partition of the time interval $\mathcal{J}$ into a set of N non-overlapping subintervals such that

$$\mathcal{J} = [0,T] = \bigcup_{k=1}^{N} [t_k, t_{k+1}].$$

Hence, the solution to (4.3) is obtained by solving an initial-value problem for each time interval T_k, where the solution is known at $t = t_k$. For a time step t_{k+1}, we denote the solution $\boldsymbol{\alpha}(t_{k+1})$ by $\boldsymbol{\alpha}_{k+1}$. The system (4.3) becomes

$$\boldsymbol{K}\boldsymbol{\alpha}_{k+1} - \int_0^{t_{k+1}} \widetilde{\boldsymbol{K}}(t_{k+1}-s)\boldsymbol{\alpha}(s)\,\mathrm{d}s = \boldsymbol{Q}_{k+1}. \tag{4.4}$$

The convolution in (4.4) can be computed, in general, using the trapezoidal rule. In fact, we have that

$$\begin{aligned}
\int_0^{t_{k+1}} \widetilde{\boldsymbol{K}}(t_{k+1}-s)\boldsymbol{\alpha}(s)\,\mathrm{d}s &= \sum_{p=1}^{k} \int_{t_p}^{t_{p+1}} \widetilde{\boldsymbol{K}}(t_{k+1}-s)\boldsymbol{\alpha}(s)\,\mathrm{d}s \\
&= \sum_{p=1}^{k-1} \int_{t_p}^{t_{p+1}} \widetilde{\boldsymbol{K}}(t_{k+1}-s)\boldsymbol{\alpha}(s)\,\mathrm{d}s + \int_{t_k}^{t_{k+1}} \widetilde{\boldsymbol{K}}(t_{k+1}-s)\boldsymbol{\alpha}(s)\,\mathrm{d}s \\
&\approx \frac{\Delta t}{2}\left\{\widetilde{\boldsymbol{K}}(t_{k+1}-t_1)\boldsymbol{\alpha}_1 + 2\sum_{p=2}^{k}\widetilde{\boldsymbol{K}}(t_{k+1}-t_p)\boldsymbol{\alpha}_p\right\} + \frac{\Delta t}{2}\widetilde{\boldsymbol{K}}(0)\boldsymbol{\alpha}_{k+1},
\end{aligned}$$

where $\boldsymbol{\alpha}_p, p < k+1$, are the known solutions from previous steps. This approximation results in a fully discretized system:

$$\boldsymbol{S}\boldsymbol{\alpha}_{k+1} = \widetilde{\boldsymbol{Q}}_{k+1},$$

where

$$\widetilde{\boldsymbol{Q}}_{k+1} = \boldsymbol{Q}_{k+1} + \frac{\Delta t}{2}\left\{\widetilde{\boldsymbol{K}}(t_{k+1}-t_1)\boldsymbol{\alpha}_1 + 2\sum_{p=2}^{k}\widetilde{\boldsymbol{K}}(t_{k+1}-t_p)\boldsymbol{\alpha}_p\right\}, \tag{4.5}$$

and the matrix $\boldsymbol{S}$ is of the form

$$\boldsymbol{S} := \boldsymbol{K} - \frac{\Delta t}{2}\widetilde{\boldsymbol{K}}(0).$$

The matrix entries depend on the particular geometry of the structure, as well as on the viscoelastic material properties. For example, specific components for this matrix can be deduced from the works of [41, 42] in the case of a viscoelastic Timoshenko beam.

We now observe that as N gets larger, the algorithm efficiency decreases since the computation of (4.5) becomes expensive due to the increasing number of elements inside the sum. To mitigate this issue, we resort to a technique provided in the works of [41, 42, 47] that allows to avoid the store and computation of the entire deformation history. More precisely, we provide a recurrence formula to only need a previous time step data.

Considering the relaxation modulus given above, let us assume, without loss of generality, that we can write them like (see for example [37]):

$$E(t) = a + be^{-t/\tau}.$$

Then, for a given time step t_{k+1} we have that

$$\dot{E}(t_{k+1}-s) = -\frac{b}{\tau}e^{-(t_{k+1}-s)/\tau} = -\frac{b}{\tau}e^{-(t_k+\Delta t-s)/\tau} = e^{-\Delta t/\tau}\dot{E}(t_k-s).$$

We remark that this multiplicative decomposition of the relaxation modulus can be extended to the full Prony series (see for instance [47]). Hence, we have

$$\widetilde{\boldsymbol{K}}(t_{k+1}-s) = \dot{E}(t_{k+1}-s)\boldsymbol{K} = e^{-\Delta t/\tau}\dot{E}(t_k-s)\boldsymbol{K} = e^{-\Delta t/\tau}\widetilde{\boldsymbol{K}}(t_k-s). \tag{4.6}$$

Applying the decomposition (4.6) in (4.5) we rewrite the right hand side $\widetilde{\boldsymbol{Q}}$ as

$$\widetilde{\boldsymbol{Q}}_{k+1} = \boldsymbol{Q}_{k+1} + \boldsymbol{g}(k),$$

where

$$\boldsymbol{g}(k) := e^{-\Delta t/\tau}\left\{\frac{\Delta t}{2}\widetilde{\boldsymbol{K}}(t_k-t_1)\boldsymbol{\alpha}_1 + \Delta t\sum_{p=2}^{k}\widetilde{\boldsymbol{K}}(t_k-t_p)\boldsymbol{\alpha}_p\right\}.$$

Note that, if we consider the calculation of $\boldsymbol{g}(k+1)$, we can reuse (4.6) in order to obtain

$$\begin{aligned}
\boldsymbol{g}(k+1) &= e^{-\Delta t/\tau}\left\{\frac{\Delta t}{2}\widetilde{\boldsymbol{K}}(t_{k+1}-t_1)\boldsymbol{\alpha}_1 + \Delta t\sum_{p=2}^{k+1}\widetilde{\boldsymbol{K}}(t_{k+1}-t_p)\boldsymbol{\alpha}_p\right\}\\
&= e^{-\Delta t/\tau}\left\{\frac{\Delta t}{2}\widetilde{\boldsymbol{K}}(t_{k+1}-t_1)\boldsymbol{\alpha}_1 + \Delta t\sum_{p=2}^{k}\widetilde{\boldsymbol{K}}(t_{k+1}-t_p)\boldsymbol{\alpha}_p + \Delta t\widetilde{\boldsymbol{K}}(0)\boldsymbol{\alpha}_{k+1}\right\}\\
&= e^{-\Delta t/\tau}\left\{e^{-\Delta t/\tau}\left[\frac{\Delta t}{2}\widetilde{\boldsymbol{K}}(t_k-t_1)\boldsymbol{\alpha}_1 + \Delta t\sum_{p=2}^{k}\widetilde{\boldsymbol{K}}(t_k-t_p)\boldsymbol{\alpha}_p\right] + \Delta t\widetilde{\boldsymbol{K}}(0)\boldsymbol{\alpha}_{k+1}\right\}\\
&= e^{-\Delta t/\tau}\left\{\boldsymbol{g}(k) + \Delta t\widetilde{\boldsymbol{K}}(0)\boldsymbol{\alpha}_{k+1}\right\}.
\end{aligned}$$

Hence, we have obtained a recurrence formula where k represents the time step t_k and the function $\boldsymbol{g}(k)$ is the cumulative additions of the history terms. The main advantage of this approach relies on the fact that for the step $k+1$, we only need to know the solution $\boldsymbol{\alpha}_k$ and the vector $\boldsymbol{g}(k)$, both stored in the k step, in order to compute $\boldsymbol{g}(k+1)$. Therefore, for each iteration, there is no need to store all the history terms, but only the data from the previous step. For nonlinear problems, the history matrix $\widetilde{\boldsymbol{K}}(t-s)$ can be written as $\dot{E}(t-s)\boldsymbol{M}$, where $\boldsymbol{M}$ is an appropriate stiffness matrix including the nonlinear terms. A recurrence formula is also possible in this case, and we refer to Section 4.1 of [41] for more details.

On the other hand, It is well known that the trapezoidal rule error is of order 2. Thus, from the semi-discrete error analysis, we have that given a semi-discrete rate of convergence $\mathcal{O}(h^r)$, we expect that the fully discrete error estimates satisfies

$$\begin{aligned} \mathsf{e}_{0,\ell}(f) &\lesssim h^{r+1} + \Delta t^2, & \mathsf{e}_{\mathbf{0},\ell}(\boldsymbol{f}) &\lesssim h^{r+1} + \Delta t^2,\\ \mathsf{e}_{1,\ell}(f) &\lesssim h^{r} + \Delta t^2, & \mathsf{e}_{\mathbf{1},\ell}(\boldsymbol{f}) &\lesssim h^{r} + \Delta t^2. \end{aligned}$$

We then choose the step size such that $\Delta t^2 \ll h^r$, for $r \geq 1$.

4.1. Timoshenko beam

We begin with an application of the developed abstract theory to a clamped linear viscoelastic Timoshenko beam. It is well known that, in the elastic case, the Timoshenko beam system lead to a parameter dependent problem, where the thickness plays the role of deteriorate the standard numerical methods, which in the viscoelastic setting is expectable as well (see [27,28] for instance). Now we will check how our abstract framework helps to avoid the locking effect for a viscoelastic formulation of this beam.

Let $\Omega := [0,L]$, where L represents the length of the beam. We consider the space of square-integrable functions $L^2(\Omega)$ with inner product $(u,v) := \int_\Omega u\,v\,\mathrm{d}x$, and its induced norm $\|f\|_{L^2(\Omega)} = \sqrt{(f,f)}$.

We introduce the space

$$\mathrm{H} = \left\{(v,\eta) \in H_0^1(\Omega) \times H_0^1(\Omega)\right\},$$

endowed with the product space seminorm

$$\|(\eta,w)\|_{\mathrm{H}}^2 := \|\eta'\|_{L^2(\Omega)}^2 + \|w'\|_{L^2(\Omega)}^2,$$

where $\zeta'(x) := \mathrm{d}\zeta/\mathrm{d}x$.

Under suitable kinematic assumptions, the constitutive equations given in (4.2) allow to obtain a viscoelastic Timoshenko beam (see for example [41]). In our case, the viscoelastic Timoshenko beam model to be analyzed is the following: Given $\ell \in [1,\infty]$, find $(w,\theta) \in L^\ell(\mathcal{J};\mathrm{H})$ such that

$$\begin{aligned} (I(x)\theta',\eta') + k_s(A(x)(\theta - w'),\eta - v') = \left(\widetilde{f},v\right) &+ \int_0^t \dot{E}(t-s)(I(x)\theta'(s),\eta')\,\mathrm{d}s\\ &+ k_s\int_0^t \dot{G}(t-s)(A(x)(\theta(s) - w'(s)),\eta - v')\,\mathrm{d}s, \end{aligned} \tag{4.7}$$

for all $(v,\eta) \in \mathrm{H}$, where w represents the displacement of the beam, θ represent the rotations, k_s is the correction factor, $E(t)$ is the relaxation modulus, $G(t) := E(t)/2(1+\nu)$ is the shear modulus, ν is the time-independent Poisson ratio, $I(x)$ is the moment of inertia of the cross-section, $A(x)$ is the area of the cross-section and $\widetilde{f}(x,t)$ is a uniform distributed transverse load.

The viscoelastic boundary value problem associated with (4.7) states that a.e. in $\mathcal{J}$:

$$\begin{aligned} -I(x)\theta'' + k_sA(x)(\theta - w') &= -\int_0^t \dot{E}(t-s)I(x)\theta''(s)\,\mathrm{d}s + k_s\int_0^t \dot{G}(t-s)A(x)(\theta(s) - w'(s))\,\mathrm{d}s && \text{in } \Omega,\\ k_sA(x)(\theta - w')' &= \widetilde{f} + k_s\int_0^t \dot{G}(t-s)(\theta(s) - w'(s))'\,\mathrm{d}s, && \text{in } \Omega,\\ w = \theta &= 0, && \text{on } \partial\Omega. \end{aligned}$$

We now proceed to rescale the formulation (4.7) to identify a family of viscoelastic problems whose limit is well-posed when the thickness of the beam goes to zero. We introduce the following classic non-dimensional parameter, characteristic of the thickness of the beam

$$\epsilon^2 = \frac{1}{L}\int_\Omega \frac{I(x)}{A(x)L^2}\,\mathrm{d}x,$$

which is assumed to be independent of time and is such that $\epsilon \in (0, \epsilon_{\max}]$.

Scaling the load as $\widetilde{f}(x,t) = \epsilon^3 f(x,t)$, with $f(x,t)$ independent of ϵ, and defining

$$\hat{I}(x) := \frac{I(x)}{\epsilon^3}, \qquad \hat{A}(x) := k_s \frac{A(x)}{\epsilon},$$

we have that (4.7) is equivalent to the following problem:

Problem 4.1. Given $f \in L^\ell(\mathcal{J}; L^2(\Omega))$, find $(\theta, w) \in L^\ell(\mathcal{J}; \mathrm{H})$ such that

$$\begin{aligned}\left(\hat{I}\theta', \eta'\right) + \frac{\epsilon^{-2}}{2(1+\nu)}\left(\hat{A}(\theta - w'), \eta - v'\right) &= (f, v)\\ &+ \int_0^t \dot{E}(t-s)\left[\left(\hat{I}\theta'(s), \eta'\right) + \frac{\epsilon^{-2}}{2(1+\nu)}\left(\hat{A}(\theta(s) - w'(s)), \eta - v'\right)\right]\mathrm{d}s,\end{aligned}$$

for all $(v, \eta) \in \mathrm{H}$.

We introduce the unit shear $\gamma \in L^\ell(\mathcal{J}; L^2(\Omega))$ as $\gamma := \frac{\epsilon^{-2}}{2(1+\nu)}\hat{A}(\theta - w')$. Hence, defining $\lambda := 2(1+\nu)\epsilon^2$, we rewrite Problem 4.1 as the following mixed formulation:

Problem 4.2. Find $(\theta, w, \gamma) \in L^\ell(\mathcal{J}; \mathrm{H} \times L^2(\Omega))$ such that

$$\begin{cases}\left(\hat{I}\theta', \eta'\right) + (\gamma, \eta - v') = (f, v) + \displaystyle\int_0^t \dot{E}(t-s)\left[\left(\hat{I}\theta'(s), \eta'\right) + (\gamma(s), \eta - v')\right]\mathrm{d}s,\\ (\theta - w', \psi) - \lambda\left(\gamma/\hat{A}, \psi\right) = 0,\end{cases}$$

for all $(v, \eta) \in \mathrm{H}$ and for all $\psi \in L^2(\Omega)$.

Now we verify that Problem 4.2 lies in the framework of the abstract setting provided in the previous section. First, note that according to our abstract framework, $\mathcal{V} := \mathrm{H}$, $\mathcal{Q} := L^2(\Omega)$, $u := (\theta, w)$, $v := (\eta, v)$, $p := \gamma$, $q := \psi$. Then, the bilinear forms $a : \mathcal{V} \times \mathcal{V} \to \mathbb{R}$ and $b : \mathcal{V} \times L^2(\varOmega) \to \mathbb{R}$, are given by

$$a((\theta, w); (\eta, v)) := \left(\hat{I}\theta', \eta'\right), \quad b((\eta, v); \gamma) := (\gamma, \eta - v'),$$

for all $(\theta, w), (\eta, v) \in \mathrm{H}$, $\gamma \in L^2(\Omega)$ a.e. in $\mathcal{J}$. It is straightforward that $a(\cdot,\cdot)$ is $\mathcal{K}$-elliptic, where $\mathcal{K}$ is the kernel of b, and $b(\cdot,\cdot)$ satisfies an inf-sup condition (see for example [4], Sect. 5). Then, from Theorem 2.7, we have

$$\|(\theta, w)\|_{L^\ell(0,t;\mathcal{V})} + \|\gamma\|_{L^\ell(0,t;L^2(\Omega))} \lesssim \|f\|_{L^\ell(0,t;L^2(\Omega))},$$

where the hidden constant is uniform in λ.

Finally, we note that using the differential equations satisfied by the solutions of the mixed formulation in the distributional sense (see for example [9], Prop. 3 for the case of a rod), the following additional regularity result holds

$$\|\theta\|_{L^\ell(0,t;H^2(\Omega))} + \|w\|_{L^\ell(0,t;H^2(\Omega))} + \|\gamma\|_{L^\ell(0,t;H^1(\Omega))} \lesssim \|f\|_{L^\ell(0,t;L^2(\Omega))}. \tag{4.8}$$

Note that by defining the form

$$B_\epsilon((\theta,w);(\eta,v)) := \Big(\hat{I}\theta',\eta'\Big) + \frac{\epsilon^{-2}}{2(1+\nu)}\Big(\hat{A}(\theta-w'),\eta-v'\Big),$$

Problem 4.1 can be written as: Given $f\in L^\ell(\mathcal{J};L^2(\Omega))$, find $(\theta,w)\in L^\ell(\mathcal{J};\mathcal{V})$ such that

$$B_\epsilon((\theta,w);(\eta,v)) = (f,v) + \int_0^t \widetilde{B}_\epsilon(t,s,(\theta(s),w(s));(\eta,v))\,\mathrm{d}s, \tag{4.9}$$

where the form $\widetilde{B}_\epsilon(\cdot,\cdot,(\cdot,\cdot);(\cdot,\cdot))$ is defined by

$$\widetilde{B}_\epsilon(t,s,(\theta(s),w(s));(\eta,v)) := \dot{E}(t-s)B_\epsilon((\theta(s),w(s));(\eta,v)).$$

Hence, (4.9) fits in the theory provided in [46]. Indeed, note that thanks to the Poincaré inequality, the form $B_\epsilon((\cdot,\cdot);(\cdot,\cdot))$ satisfies (see for instance [4])

$$\|(\eta,v)\|_{\mathcal{V}} \lesssim [B_\epsilon((\eta,v);(\eta,v))]^{1/2} \lesssim \big(1+\epsilon^{-2}\big)\|(\eta,v)\|_{\mathcal{V}},$$

and consequently, the form $\widetilde{B}_\epsilon(\cdot,\cdot,(\cdot,\cdot);(\cdot,\cdot))$ satisfies a similarity condition in the sense of Assumption 1 from [46], *i.e.*,

$$\Big|\widetilde{B}_\epsilon(t,s,(\theta(s),w(s));(\eta,v))\Big| \lesssim \big(1+\epsilon^{-2}\big)\|(\eta,v)\|_{\mathcal{V}}.$$

Therefore, resorting to the differential equations satisfied by the solution of (4.9), we have that

$$\|\theta\|_{L^\ell(0,t;H^2(\Omega))} + \|w\|_{L^\ell(0,t;H^2(\Omega))} + \epsilon^{-2}\|\theta-w'\|_{L^\ell(0,t;H^1(\Omega))} \lesssim \|f\|_{L^\ell(0,t;L^2(\Omega))}, \tag{4.10}$$

holds, where the hidden constant is independent of ϵ.

The importance of including this problem is that it will allow to improve the error estimates provided by our numerical scheme using weaker norms (see Sect. 4.1.1 below).

4.1.1. Finite element analysis

Now our task is to analyze a conforming finite element semi-discretization for the beam mixed formulation provided previously. The main goal is to derive error estimates, independent of the thickness parameter. As a starting point, consider a finite partition $\mathscr{T}_h = \big\{\Omega_i\big\}_{i=1}^n$ of the computational domain Ω such that $\Omega_i =]x_{i-1},x_i[$, with length $h_i = x_i - x_{i-1}$, and satisfying $\bigcap_{i=1}^n \Omega_i = \emptyset$ and $\Omega = \bigcup_{i=1}^n \overline{\Omega}_i$, $i=1,\dots,n$. The maximum interval length is denoted by $h = \max_{1\le i\le n} h_i$.

The approximations will be based in the following finite element spaces:

$$\begin{aligned}\mathrm{H}_h &:= \big\{v\in H_0^1(\Omega) : v_{|\Omega_i}\in\mathcal{P}_1(\Omega_i),\ \Omega_i\in\mathscr{T}_h\big\},\\ \mathcal{Q}_h &:= \big\{q\in L^2(\Omega) : q_{|\Omega_i}\in\mathcal{P}_0(\Omega_i),\ \Omega_i\in\mathscr{T}_h\big\},\end{aligned}$$

where $\mathcal{V}_h := \mathrm{H}_h\times\mathrm{H}_h$ approximates the displacement and rotations, and the shear stress is approximated with the piecewise constants of $\mathcal{Q}_h$.

We also recall the Lagrange interpolant $\mathcal{L}_h : C(\overline{\Omega}) \to \mathrm{H}_h$ and the classic L^2 projector onto constants $\Pi_h : L^2(\Omega)\to\mathcal{Q}_h$, such that the estimates

$$\|u-\mathcal{L}_h u\|_{H^1(\Omega)} \lesssim h|u|_{H^2(\Omega)}, \quad \text{and} \quad \|v-\Pi_h(v)\|_{L^2(\Omega)} \lesssim h|v|_{H^1(\Omega)} \tag{4.11}$$

hold (see [17], Sect. 1.1.3 and [17], Sect. 1.6.3, respectively).

From the above estimates, it follows that the more regular spaces required in the abstract setting are given by

$$\mathcal{V}_{++} := H^2(\Omega)\times H^2(\Omega) \qquad \text{and} \qquad \mathcal{Q}_{++} := H^1(\Omega).$$

Now, the corresponding semi-discrete counterpart of Problem 4.2 is given as follows:

Problem 4.3. Find $(\theta_h, w_h, \gamma_h) \in L^\ell(\mathcal{J}; \mathcal{V}_h \times \mathcal{Q}_h)$ such that

$$\begin{cases} \left(\hat{I}\theta_h', \eta'\right) + (\gamma_h, \eta - v') = (f, v) + \displaystyle\int_0^t \dot{E}(t-s)\left[\left(\hat{I}\theta_h'(s), \eta'\right) + (\gamma_h(s), \eta - v')\right] \mathrm{d}s, \\ (\theta_h - w_h', \psi) - \lambda\left(\gamma_h/\hat{A}, \psi\right) = 0, \end{cases}$$

for all $(v, \eta) \in \mathcal{V}_h$ and for all $\psi \in \mathcal{Q}_h$.

Following Section 5 of [4], we observe that the restriction of $a(\cdot,\cdot)$ to $\mathcal{V}_h$ satisfies the ellipticity condition in $\mathcal{K}_h$, while the restriction $b(\cdot,\cdot)$ to $\mathcal{V}_h \times \mathcal{Q}_h$ satisfies an inf-sup condition. Thus, applying Theorem 3.3 we obtain that

$$\begin{aligned} \|(\theta, w) - &(\theta_h, w_h)\|_{L^\ell(0,t;\mathcal{V})} + \|\gamma - \gamma_h\|_{L^\ell(0,t;L^2(\Omega))} \\ &\lesssim \inf_{(\eta,v)\in\mathcal{V}_h} \|(\theta, w) - (\eta, v)\|_{L^\ell(0,t;\mathcal{V})} + \inf_{\psi\in\mathcal{Q}_h} \|\gamma - \psi\|_{L^\ell(0,t;L^2(\Omega))}, \end{aligned} \tag{4.12}$$

where the hidden constant is independent of h and λ.

Hence, we have the following convergence rate for the semi-discrete mixed Problem 4.3.

Proposition 4.4. *Let $(\theta, w, \gamma) \in L^\ell(\mathcal{J}; H \times L^2(\Omega))$ and $(\theta_h, w_h, \gamma_h) \in L^\ell(\mathcal{J}; \mathcal{V}_h \times \mathcal{Q}_h)$ be the solutions of Problems 4.2 and 4.3, respectively. Then, if $f \in L^\ell(\mathcal{J}; L^2(\Omega))$, we have*

$$\|(\theta, w) - (\theta_h, w_h)\|_{L^\ell(0,t;\mathcal{V})} + \|\gamma - \gamma_h\|_{L^\ell(0,t;L^2(\Omega))} \lesssim h\|f\|_{L^\ell(0,t;L^2(\Omega))},$$

where the hidden constant is independent of h and λ.

Proof. The proof follows from (4.12), the error estimates (4.8), and estimates (4.11). □

In what follows, we will consider the dual-backward version of Problem 4.3 to obtain an additional error estimate. Note that the estimate for γ is not possible to be improved since the choice of a space less regular than $L^2(\Omega)$ is not available. Also, note that the abstract setting suggests that $(\mathcal{V}_-)' = \mathcal{V}_+' = L^2(\Omega) \times L^2(\Omega)$. However, we can take advantage of the connection between the proposed mixed formulation and a reduced integration scheme. Indeed, it is known that for Timoshenko beams, in order to prevent locking, the following condition is enforced

$$\Pi_h(\theta_h) - w_h' = 0.$$

The space integrals involving the shear terms are computed using a Gauss numerical quadrature scheme with k points per element on the quantities $(\theta_h - w_h)(\eta - v)$.

The following result summarizes this approach, stated in Proposition 7.2.5 from [10] as a direct consequence of a more general approach given in [6].

Theorem 4.5. *For any continuous piecewise-$\mathbb{P}_k$ function θ, inside each element $\Pi_h(\theta)$ is the unique $\mathbb{P}_{k-1}$ polynomial that takes the same values as θ at the k points of the Gauss numerical quadrature.*

Following this approach and with the help of Π_h, together with the second equation of Problem 4.3, we have

$$\gamma_h := \frac{\epsilon^{-2}}{2(1+\nu)} \hat{A}(\Pi_h(\theta_h) - w_h'). \tag{4.13}$$

By replacing this approximation in the corresponding first equation of Problem 4.3 gives that the solutions (θ_h, w_h) of Problem 4.3 solves: Find $(\theta_h, w_h) \in L^\ell(\mathcal{J}; \mathcal{V}_h)$ such that

$$\begin{aligned} \left(\hat{I}\theta_h', \eta'\right) + \frac{\epsilon^{-2}}{2(1+\nu)}\left(\hat{A}\Pi_h(\theta_h - w_h'), \eta - v'\right) - \int_0^t \dot{E}(t-s)\Big[\left(\hat{I}\theta_h'(s), \eta'\right) \\ + \frac{\epsilon^{-2}}{2(1+\nu)}\left(\hat{A}\Pi_h(\theta_h(s) - w_h'(s)), \eta - v'\right)\Big] \mathrm{d}s = (f, v), \end{aligned} \tag{4.14}$$

for all $(v,\eta)\in\mathcal{V}_h$, which corresponds to a reduced integration scheme.

Now we are in position to improve the convergence rate of the scheme.

Proposition 4.6. *Let $(\theta,w)\in\mathcal{V}$ and $(\theta_h,w_h)\in\mathcal{V}_h$ be the solutions to (4.9) and (4.14). Denote by $\mathsf{e}_\theta=\theta-\theta_h$ and $\mathsf{e}_w=w-w_h$ the errors. Then it follows that*

$$\|(\theta,w)-(\theta_h,w_h)\|_{L^\ell(0,t;L^2(\Omega)^2)}\lesssim h^2\|f\|_{L^\ell(0,t;L^2(\Omega))},$$

where the hidden constant is independent of h and λ.

Proof. Following the construction of the dual-backward problem (3.6) and using the same variable substitution to write it in forward form as in (3.7), we construct a forward form of the dual version of (4.9) satisfying all the necessary stability and regularity properties such as (4.10).

Given $\tau\in\mathcal{J}$ and for any $(f_+,g_+),\in L^r(0,\tau;\mathcal{V}_+')$, we consider the dual problem: Find $(\rho,\mu)\in L^r(0,\tau;\mathcal{V})$ such that a.e. in $[0,\tau]$,

$$B_\epsilon((\eta,v);(\rho,\mu))=\langle(f_+,g_+),(\eta,v)\rangle_{\mathcal{V}}+\int_t^\tau\widetilde{B}_\epsilon(s,t)((\eta,v);(\rho(s),\mu(s)))\,\mathrm{d}s,$$

for all $(\eta,v)\in\mathcal{V}$. Note that this is slightly more general version of (4.9) because of the presence of g_+. From (4.10) we have

$$\|\rho\|_{L^\ell(0,t;H^2(\Omega))}+\|\mu\|_{L^\ell(0,t;H^2(\Omega))}\lesssim\|(f_+,g_+)\|_{L^\ell(0,t;L^2(\Omega)^2)}. \tag{4.15}$$

Following the arguments from Theorem 3.4, we take time dependent test functions $(\eta(t),v(t))\in L^\ell(0,\tau;\mathcal{V})$, integrate in $[0,\tau]$, and interchange the order of integration in order to have

$$\int_0^\tau\langle(f_+,g_+),(\eta(t),v(t))\rangle_{\mathcal{V}}=\int_0^\tau\left\{B_\epsilon((\eta(t),v(t));(\rho(t),\mu(t)))-\int_0^t\widetilde{B}_\epsilon(t,s;(\eta(s),v(s));(\rho(t),\mu(t)))\,\mathrm{d}s\right\}\mathrm{d}t.$$

Setting $(\eta(t),v(t))=(\mathsf{e}_\theta(t),\mathsf{e}_w(t))$ and taking

$$(f_+(t),g_+(t))=z(t)(e_\theta(t),e_w(t))\|(e_\theta(t),e_w(t))\|^{-1}_{L^2(\Omega)^2},$$

we obtain

$$\begin{aligned}\int_0^\tau z(t)\|(\mathsf{e}_\theta(t),\mathsf{e}_w(t))\|_{L^2(\Omega)^2}=\int_0^\tau&\{B_\epsilon((\mathsf{e}_\theta(t),\mathsf{e}_w(t))\ (\rho(t),\mu(t)))\\&-\int_0^t\widetilde{B}_\epsilon(t,s;(\mathsf{e}_\theta(s),\mathsf{e}_w(s));(\rho(t),\mu(t)))\,\mathrm{d}s\right\}\mathrm{d}t.\end{aligned} \tag{4.16}$$

Since $(\theta_h,w_h)\in\mathcal{V}_h$ is the solution of (4.14) (resp. Problem 4.3), this pair also solves the corresponding discrete version of (4.9). Hence we use its error equation in order to have, for all $(\rho_h,\mu_h)\in\mathcal{V}_h$, the following identity

$$B_\epsilon((\mathsf{e}_\theta,\mathsf{e}_w);(\rho_h,\mu_h))=\int_0^t\widetilde{B}_\epsilon(t,s)((\mathsf{e}_\theta(s),\mathsf{e}_w(s));(\rho_h,\mu_h))\,\mathrm{d}s=0. \tag{4.17}$$

Then, setting $\mathsf{e}_\rho:=\rho-\rho_h$ and $\mathsf{e}_\mu=\mu-\mu_h$, from (4.16) and (4.17) we obtain

$$\int_0^\tau z(t)\|(\mathsf{e}_\theta,\mathsf{e}_w)\|_{L^2(\Omega)^2}=\int_0^\tau\left\{B_\epsilon((\mathsf{e}_\theta,\mathsf{e}_w)\ (\mathsf{e}_\rho,\mathsf{e}_\mu))-\int_0^t\widetilde{B}_\epsilon(t,s;(\mathsf{e}_\theta(s),\mathsf{e}_w(s));(\mathsf{e}_\rho,\mathsf{e}_\mu))\,\mathrm{d}s\right\}\mathrm{d}t. \tag{4.18}$$

Here, we observe that the form $B_\epsilon((\cdot,\cdot);(\cdot,\cdot))$ satisfy the following relation

$$B_\epsilon((\mathsf{e}_\theta,\mathsf{e}_w)\ (\mathsf{e}_\rho,\mathsf{e}_\mu))=(\mathsf{e}_\theta',\mathsf{e}_\theta')+\frac{\epsilon^{-2}}{2(1+\nu)}((\theta-w')-(\theta_h-w_h'),(\rho-\rho_h)-(\mu'-\mu_h')),$$

with a similar result for $\widetilde{B}_\epsilon(\cdot,\cdot,(\cdot,\cdot);(\cdot,\cdot))$. Then, Hölder's inequality and Lemma 2.4 allow us to obtain

$$\begin{aligned}\|(\mathsf{e}_\theta,\mathsf{e}_w)\|_{L^\ell(0,\tau;L^2(\Omega)^2)} \lesssim \big(\|(\mathsf{e}_\theta,\mathsf{e}_w)\|_{L^\ell(0,\tau;\mathcal{V})} + \|\mathsf{e}_\gamma\|_{L^\ell(0,\tau;L^2(\Omega))}\big)\\ \times\big(\|\mathsf{e}_\rho\|_{L^r(0,\tau;H^1(\Omega))} + \|\mathsf{e}_\mu\|_{L^r(0,\tau;H^1(\Omega))}\big).\end{aligned} \tag{4.19}$$

Hence, the desired estimate follows by taking $\tau = t$ in (4.19) and Proposition 4.4, together with (4.13), (4.15), and estimate (4.11). □

4.1.2. Numerical tests

Now we report a series of numerical tests in order to confirm our theoretical results. The algorithms have been implemented in FEniCS [1].

In the following, the experimental nature of the relaxation modulus is replaced by assumed values of spring constants and viscosity parameters in order to consider the *Standard Linear Solid model* (SLS). The relaxation and shear modulus for this material are given by the truncated Prony series:

$$E(t) = \frac{k_1k_2}{k_1+k_2} + \left(k_1 - \frac{k_1k_2}{k_1+k_2}\right)e^{-t/\tau}, \qquad G(t) = \frac{E(t)}{2(1+\nu)},$$

where $\tau = \eta/(k_1+k_2)$. We will consider $\nu = 0.35$ in all the experiments.

We consider the physical parameters considered in [38]. More precisely, we consider an homogeneous rectangular beam of length $L = 4\,\mathrm{m}$, with base $b = 0.08\,\mathrm{m}$ and thickness d. The corresponding moment of inertia is $I = 0.08\,d^3/12\,\mathrm{m}^4$ and the cross section area is $A = 0.08\,d\,\mathrm{m}^2$. We set the thickness parameter as $\epsilon^2 = I/AL^2$.

On the other hand, the creep load for the beam is $f(\widetilde{x},t) = 8\,H(t)\,\mathrm{N/m}$, where $\widetilde{x} = x/L$. This case considers the SLS parameters $k_1 = 9.8\times10^7\,\mathrm{N/m^2}$, $k_2 = 2.44\times10^7\,\mathrm{N/m^2}$ and $\eta = 2.74\cdot10^8\,\mathrm{N{\cdot}s/m^2}$. The observation time is $10\,\mathrm{s}$ with step size $\Delta t = 0.002$. The quasi-static analytical solution is obtained by means of the corresponding principle [37], and is given by (see for example [50]):

$$\begin{aligned} w(\widetilde{x},t) &= \widetilde{f}(\widetilde{x},t)\left[\frac{L^4}{24I}\big(\widetilde{x} - 2\widetilde{x}^3 + \widetilde{x}^4\big) + \frac{L^2}{2G_0A}\widetilde{x}(1-\widetilde{x})\right]J(t),\\ \theta(\widetilde{x},t) &= \widetilde{f}(\widetilde{x},t)\left[\frac{L^3}{24I}\big(1 - 6\widetilde{x}^2 + 4\widetilde{x}^3\big)\right]J(t),\end{aligned}$$

where $\widetilde{f}(\widetilde{x},t) = \epsilon^3 f(\widetilde{x},t)$, $G_0 = k_s/2(1+\nu)$ and $J(t)$ is the creep compliance computed from $E(t)$.

Tables 1–3 report the experimental error when $\ell = 1,2,\infty$, for the transverse displacement w, the rotation θ and the shear γ in the L^2 norm, whereas Tables 4–5 show the energy norm for the corresponding history behavior. Although the measured error for each mesh size is different between the computed norms, we observe that our method recovers the predicted convergence rates for the implemented finite elements. Since we are considering a small time step, the difference between the errors for different choices of ℓ is almost non-existent. This, together with the fact that the number of DOF's considered is not large, confirms the locking-free nature of the proposed method. We end the test by depicting a comparison between the maximum deflection of w and w_h when $d = 0.001\,\mathrm{m}$ in Figure 1. It notes that the method predicts accurately the viscoelastic behavior of the structure, compared with the exact creep compliance.

4.2. Reissner–Mindlin plate

Now we go beyond our theory, considering a mixed formulation for a Reissner–Mindlin plate. As it happens in the Timoshenko beam model, the Reissner–Mindlin plate model depends strongly on the thickness of the structure, leading to the locking phenomenon for certain numerical methods. In order to avoid this drawback, approaches such as the MITC elements (see for example [19]) are well established.

TABLE 1. Computed error values in $L^2(\Omega)$ and experimental rates of convergence for the transverse displacement w in a fully clamped viscoelastic beam.

		$d = 10^{-1}$ m		$d = 10^{-2}$ m		$d = 10^{-3}$ m	
DOF	h	$\mathtt{e}_{0,1}(w)$	$\mathtt{r}_{0,1}(w)$	$\mathtt{e}_{0,1}(w)$	$\mathtt{r}_{0,1}(w)$	$\mathtt{e}_{0,1}(w)$	$\mathtt{r}_{0,1}(w)$
32	0.400	5.5631e−02	–	5.6071e−02	–	5.6075e−02	–
62	0.200	1.4032e−02	1.99	1.4143e−02	1.99	1.4144e−02	1.99
92	0.133	6.2466e−03	2.00	6.2961e−03	2.00	6.2966e−03	2.00
122	0.100	3.5157e−03	2.00	3.5435e−03	2.00	3.5438e−03	2.00
152	0.080	2.2506e−03	2.00	2.2684e−03	2.00	2.2686e−03	2.00
182	0.067	1.5631e−03	2.00	1.5755e−03	2.00	1.5756e−03	2.00
DOF	h	$\mathtt{e}_{0,2}(w)$	$\mathtt{r}_{0,2}(w)$	$\mathtt{e}_{0,2}(w)$	$\mathtt{r}_{0,2}(w)$	$\mathtt{e}_{0,2}(w)$	$\mathtt{r}_{0,2}(w)$
32	0.400	5.5631e−02	–	5.6071e−02	–	5.6075e−02	–
62	0.200	1.4032e−02	1.99	1.4143e−02	1.99	1.4144e−02	1.99
92	0.133	6.2466e−03	2.00	6.2961e−03	2.00	6.2966e−03	2.00
122	0.100	3.5157e−03	2.00	3.5435e−03	2.00	3.5438e−03	2.00
152	0.080	2.2506e−03	2.00	2.2684e−03	2.00	2.2686e−03	2.00
182	0.067	1.5631e−03	2.00	1.5755e−03	2.00	1.5756e−03	2.00
DOF	h	$\mathtt{e}_{0,\infty}(w)$	$\mathtt{r}_{0,\infty}(w)$	$\mathtt{e}_{0,\infty}(w)$	$\mathtt{r}_{0,\infty}(w)$	$\mathtt{e}_{0,\infty}(w)$	$\mathtt{r}_{0,\infty}(w)$
32	0.400	5.5631e−02	–	5.6071e−02	–	5.6075e−02	–
62	0.200	1.4032e−02	1.99	1.4143e−02	1.99	1.4144e−02	1.99
92	0.133	6.2466e−03	2.00	6.2961e−03	2.00	6.2966e−03	2.00
122	0.100	3.5156e−03	2.00	3.5435e−03	2.00	3.5438e−03	2.00
152	0.080	2.2505e−03	2.00	2.2684e−03	2.00	2.2686e−03	2.00
182	0.067	1.5631e−03	2.00	1.5754e−03	2.00	1.5756e−03	2.00

TABLE 2. Computed error values in $L^2(\Omega)$ and experimental rate of convergence of the rotation θ in a fully clamped viscoelastic beam.

		$d = 10^{-1}$ m		$d = 10^{-2}$ m		$d = 10^{-3}$ m	
DOF	h	$\mathtt{e}_{0,1}(\theta)$	$\mathtt{r}_{0,1}(\theta)$	$\mathtt{e}_{0,1}(\theta)$	$\mathtt{r}_{0,1}(\theta)$	$\mathtt{e}_{0,1}(\theta)$	$\mathtt{r}_{0,1}(\theta)$
32	0.400	4.5607e−02	–	4.5607e−02	–	4.5607e−02	–
62	0.200	1.1443e−02	1.99	1.1443e−02	1.99	1.1443e−02	1.99
92	0.133	5.0889e−03	2.00	5.0889e−03	2.00	5.0889e−03	2.00
122	0.100	2.8631e−03	2.00	2.8631e−03	2.00	2.8631e−03	2.00
152	0.080	1.8326e−03	2.00	1.8326e−03	2.00	1.8326e−03	2.00
182	0.067	1.2726e−03	2.00	1.2726e−03	2.00	1.2726e−03	2.00
DOF	h	$\mathtt{e}_{0,2}(\theta)$	$\mathtt{r}_{0,2}(\theta)$	$\mathtt{e}_{0,2}(\theta)$	$\mathtt{r}_{0,2}(\theta)$	$\mathtt{e}_{0,2}(\theta)$	$\mathtt{r}_{0,2}(\theta)$
32	0.400	4.5607e−02	–	4.5607e−02	–	4.5607e−02	–
62	0.200	1.1443e−02	1.99	1.1443e−02	1.99	1.1443e−02	1.99
92	0.133	5.0890e−03	2.00	5.0890e−03	2.00	5.0890e−03	2.00
122	0.100	2.8632e−03	2.00	2.8632e−03	2.00	2.8632e−03	2.00
152	0.080	1.8326e−03	2.00	1.8326e−03	2.00	1.8326e−03	2.00
182	0.067	1.2727e−03	2.00	1.2727e−03	2.00	1.2727e−03	2.00
DOF	h	$\mathtt{e}_{0,\infty}(\theta)$	$\mathtt{r}_{0,\infty}(\theta)$	$\mathtt{e}_{0,\infty}(\theta)$	$\mathtt{r}_{0,\infty}(\theta)$	$\mathtt{e}_{0,\infty}(\theta)$	$\mathtt{r}_{0,\infty}(\theta)$
32	0.400	4.5607e−02	–	4.5607e−02	–	4.5607e−02	–
62	0.200	1.1443e−02	1.99	1.1443e−02	1.99	1.1443e−02	1.99
92	0.133	5.0889e−03	2.00	5.0889e−03	2.00	5.0889e−03	2.00
122	0.100	2.8631e−03	2.00	2.8631e−03	2.00	2.8631e−03	2.00
152	0.080	1.8325e−03	2.00	1.8325e−03	2.00	1.8325e−03	2.00
182	0.067	1.2726e−03	2.00	1.2726e−03	2.00	1.2726e−03	2.00

TABLE 3. Error values and experimental rate of convergence of the shear γ in a fully clamped viscoelastic beam.

		$d = 10^{-1}$ m		$d = 10^{-2}$ m		$d = 10^{-3}$ m	
DOF	h	$\mathtt{e}_{0,1}(\gamma)$	$\mathtt{r}_{0,1}(\gamma)$	$\mathtt{e}_{0,1}(\gamma)$	$\mathtt{r}_{0,1}(\gamma)$	$\mathtt{e}_{0,1}(\gamma)$	$\mathtt{r}_{0,1}(\gamma)$
32	0.400	1.0000e−01	–	1.0000e−01	–	1.0000e−01	–
62	0.200	5.0000e−02	1.00	5.0000e−02	1.00	5.0000e−02	1.00
92	0.133	3.3333e−02	1.00	3.3333e−02	1.00	3.3333e−02	1.00
122	0.100	2.5000e−02	1.00	2.5000e−02	1.00	2.5000e−02	1.00
152	0.080	2.0000e−02	1.00	2.0000e−02	1.00	2.0000e−02	1.00
182	0.067	1.6667e−02	1.00	1.6667e−02	1.00	1.6667e−02	1.00
DOF	h	$\mathtt{e}_{0,2}(\gamma)$	$\mathtt{r}_{0,2}(\gamma)$	$\mathtt{e}_{0,2}(\gamma)$	$\mathtt{r}_{0,2}(\gamma)$	$\mathtt{e}_{0,2}(\gamma)$	$\mathtt{r}_{0,2}(\gamma)$
32	0.400	1.0000e−01	–	1.0000e−01	–	1.0000e−01	–
62	0.200	5.0000e−02	1.00	5.0000e−02	1.00	5.0000e−02	1.00
92	0.133	3.3333e−02	1.00	3.3333e−02	1.00	3.3333e−02	1.00
122	0.100	2.5000e−02	1.00	2.5000e−02	1.00	2.5000e−02	1.00
152	0.080	2.0000e−02	1.00	2.0000e−02	1.00	2.0000e−02	1.00
182	0.067	1.6667e−02	1.00	1.6667e−02	1.00	1.6667e−02	1.00
DOF	h	$\mathtt{e}_{0,\infty}(\gamma)$	$\mathtt{r}_{0,\infty}(\gamma)$	$\mathtt{e}_{0,\infty}(\gamma)$	$\mathtt{r}_{0,\infty}(\gamma)$	$\mathtt{e}_{0,\infty}(\gamma)$	$\mathtt{r}_{0,\infty}(\gamma)$
32	0.400	1.0000e−01	–	1.0000e−01	–	1.0000e−01	–
62	0.200	5.0000e−02	1.00	5.0000e−02	1.00	5.0000e−02	1.00
92	0.133	3.3333e−02	1.00	3.3333e−02	1.00	3.3333e−02	1.00
122	0.100	2.5000e−02	1.00	2.5000e−02	1.00	2.5000e−02	1.00
152	0.080	2.0000e−02	1.00	2.0000e−02	1.00	2.0000e−02	1.00
182	0.067	1.6667e−02	1.00	1.6667e−02	1.00	1.6667e−02	1.00

TABLE 4. Computed error values in $H^1(\Omega)$ and experimental rates of convergence for the transverse displacement w in a fully clamped viscoelastic beam.

		$d = 10^{-1}$ m		$d = 10^{-2}$ m		$d = 10^{-3}$ m	
DOF	h	$\mathtt{e}_{1,1}(w)$	$\mathtt{r}_{1,1}(w)$	$\mathtt{e}_{1,1}(w)$	$\mathtt{r}_{1,1}(w)$	$\mathtt{e}_{1,1}(w)$	$\mathtt{r}_{1,1}(w)$
32	0.400	1.8668e−01	–	1.8799e−01	–	1.8800e−01	–
62	0.200	9.2999e−02	1.01	9.3651e−02	1.01	9.3658e−02	1.01
92	0.133	6.1957e−02	1.00	6.2391e−02	1.00	6.2395e−02	1.00
122	0.100	4.6456e−02	1.00	4.6782e−02	1.00	4.6785e−02	1.00
152	0.080	3.7161e−02	1.00	3.7421e−02	1.00	3.7424e−02	1.00
182	0.067	3.0965e−02	1.00	3.1183e−02	1.00	3.1185e−02	1.00
DOF	h	$\mathtt{e}_{1,2}(w)$	$\mathtt{r}_{1,2}(w)$	$\mathtt{e}_{1,2}(w)$	$\mathtt{r}_{1,2}(w)$	$\mathtt{e}_{1,2}(w)$	$\mathtt{r}_{1,2}(w)$
32	0.400	1.8668e−01	–	1.8799e−01	–	1.8800e−01	–
62	0.200	9.2999e−02	1.01	9.3651e−02	1.01	9.3658e−02	1.01
92	0.133	6.1957e−02	1.00	6.2391e−02	1.00	6.2395e−02	1.00
122	0.100	4.6456e−02	1.00	4.6782e−02	1.00	4.6785e−02	1.00
152	0.080	3.7161e−02	1.00	3.7421e−02	1.00	3.7424e−02	1.00
182	0.067	3.0965e−02	1.00	3.1183e−02	1.00	3.1185e−02	1.00
DOF	h	$\mathtt{e}_{1,\infty}(w)$	$\mathtt{r}_{1,\infty}(w)$	$\mathtt{e}_{1,\infty}(w)$	$\mathtt{r}_{1,\infty}(w)$	$\mathtt{e}_{1,\infty}(w)$	$\mathtt{r}_{1,\infty}(w)$
32	0.400	1.8668e−01	–	1.8799e−01	–	1.8800e−01	–
62	0.200	9.2999e−02	1.01	9.3651e−02	1.01	9.3658e−02	1.01
92	0.133	6.1957e−02	1.00	6.2391e−02	1.00	6.2395e−02	1.00
122	0.100	4.6456e−02	1.00	4.6782e−02	1.00	4.6785e−02	1.00
152	0.080	3.7161e−02	1.00	3.7421e−02	1.00	3.7424e−02	1.00
182	0.067	3.0965e−02	1.00	3.1183e−02	1.00	3.1185e−02	1.00

TABLE 5. Computed error values in $H^1(\Omega)$ and experimental rate of convergence of the rotation θ in a fully clamped viscoelastic beam.

		$d = 10^{-1}$ m		$d = 10^{-2}$ m		$d = 10^{-3}$ m	
DOF	h	$\mathtt{e}_{1,1}(\theta)$	$\mathtt{r}_{1,1}(\theta)$	$\mathtt{e}_{1,1}(\theta)$	$\mathtt{r}_{1,1}(\theta)$	$\mathtt{e}_{1,1}(\theta)$	$\mathtt{r}_{1,1}(\theta)$
32	0.400	2.2271e−01	–	2.2271e−01	–	2.2271e−01	–
62	0.200	1.1169e−01	1.00	1.1169e−01	1.00	1.1169e−01	1.00
92	0.133	7.4502e−02	1.00	7.4502e−02	1.00	7.4502e−02	1.00
122	0.100	5.5888e−02	1.00	5.5888e−02	1.00	5.5888e−02	1.00
152	0.080	4.4714e−02	1.00	4.4714e−02	1.00	4.4714e−02	1.00
182	0.067	3.7264e−02	1.00	3.7264e−02	1.00	3.7264e−02	1.00
DOF	h	$\mathtt{e}_{1,2}(\theta)$	$\mathtt{r}_{1,2}(\theta)$	$\mathtt{e}_{1,2}(\theta)$	$\mathtt{r}_{1,2}(\theta)$	$\mathtt{e}_{1,2}(\theta)$	$\mathtt{r}_{1,2}(\theta)$
32	0.400	2.2271e−01	–	2.2271e−01	–	2.2271e−01	–
62	0.200	1.1169e−01	1.00	1.1169e−01	1.00	1.1169e−01	1.00
92	0.133	7.4502e−02	1.00	7.4502e−02	1.00	7.4502e−02	1.00
122	0.100	5.5888e−02	1.00	5.5888e−02	1.00	5.5888e−02	1.00
152	0.080	4.4714e−02	1.00	4.4714e−02	1.00	4.4714e−02	1.00
182	0.067	3.7264e−02	1.00	3.7264e−02	1.00	3.7264e−02	1.00
DOF	h	$\mathtt{e}_{1,\infty}(\theta)$	$\mathtt{r}_{1,\infty}(\theta)$	$\mathtt{e}_{1,\infty}(\theta)$	$\mathtt{r}_{1,\infty}(\theta)$	$\mathtt{e}_{1,\infty}(\theta)$	$\mathtt{r}_{1,\infty}(\theta)$
32	0.400	2.2271e−01	–	2.2271e−01	–	2.2271e−01	–
62	0.200	1.1169e−01	1.00	1.1169e−01	1.00	1.1169e−01	1.00
92	0.133	7.4502e−02	1.00	7.4502e−02	1.00	7.4502e−02	1.00
122	0.100	5.5888e−02	1.00	5.5888e−02	1.00	5.5888e−02	1.00
152	0.080	4.4714e−02	1.00	4.4714e−02	1.00	4.4714e−02	1.00
182	0.067	3.7264e−02	1.00	3.7264e−02	1.00	3.7264e−02	1.00

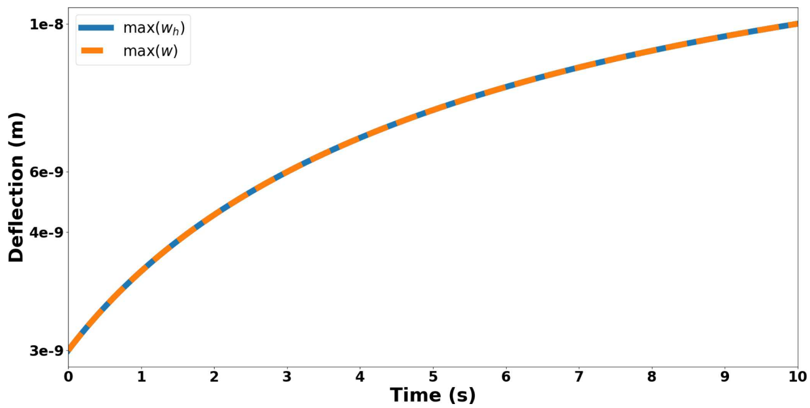

FIGURE 1. Comparison between exact and discrete maximum deflections, w and w_h, in the viscoelastic Timoshenko beam, where $d = 10^{-3}$ m and $\Delta t = 0.002$.

For our purposes, we consider that the plate is clamped. Let us recall the following standard definitions

$$\operatorname{div} \boldsymbol{\eta} := \partial_1\eta_1 + \partial_2\eta_2, \quad \operatorname{rot} \boldsymbol{\eta} := \partial_1\eta_2 - \partial_2\eta_1, \qquad \nabla v := (\partial_1 v, \partial_2 v)^{\mathrm{t}},$$
$$\operatorname{curl} v := (\partial_2 v, -\partial_1 v)^{\mathrm{t}}, \quad \mathbf{div}\,\boldsymbol{\tau} := \begin{pmatrix} \partial_1\tau_{11} + \partial_2\tau_{12} \\ \partial_1\tau_{21} + \partial_2\tau_{22} \end{pmatrix}, \quad \nabla\boldsymbol{\eta} := \begin{pmatrix} \partial_1\eta_1 & \partial_2\eta_1 \\ \partial_1\eta_2 & \partial_2\eta_2 \end{pmatrix},$$

where $\mathtt{t}$ denotes the transpose operator.

For $0 < d \leq 1$, let $\Omega \times (-\frac{d}{2}, \frac{d}{2})$ be the region occupied by the plate, where $\Omega \subset \mathbb{R}^2$ is an open and convex domain with Lipschitz boundary $\partial\Omega$. We denote the inner product in L^2 for tensor, vector and scalar functions by $(\cdot, \cdot)$.

From the constitutive relations (4.2) and inspired by [19], we propose the following viscoelastic Reissner–Mindlin plate system

$$\begin{cases} -\operatorname{\mathbf{div}} \mathbb{C}\boldsymbol{\varepsilon}(\boldsymbol{\theta}) - \boldsymbol{\gamma} = -\boldsymbol{f} - \displaystyle\int_0^t \dot{E}(t-s)\{\operatorname{\mathbf{div}} \mathbb{C}\boldsymbol{\varepsilon}(\boldsymbol{\theta}(s)) + \boldsymbol{\gamma}(s)\}\,\mathrm{d}s, & \text{in } \Omega, \\ -\operatorname{div} \boldsymbol{\gamma} = g - \displaystyle\int_0^t \dot{E}(t-s) \operatorname{div} \boldsymbol{\gamma}(s)\,\mathrm{d}s, & \text{in } \Omega, \\ \boldsymbol{\gamma} = \dfrac{\kappa}{d^2}(\nabla w - \boldsymbol{\theta}), & \text{in } \Omega, \\ w = 0, \quad \boldsymbol{\theta} = 0, & \text{on } \partial\Omega, \end{cases} \tag{4.20}$$

where $\kappa := k_s/2(1+\nu)$, g is the scaled distributed transverse load, $\boldsymbol{f}$ is a volume density load, and $\mathbb{C}$ is a unit elastic modulus, whose action is given by

$$\mathbb{C}\boldsymbol{\tau} := \frac{1}{12(1-\nu^2)}[(1-\nu)\boldsymbol{\tau} + \nu \operatorname{tr}(\boldsymbol{\tau})\mathbf{I}], \quad \boldsymbol{\tau} \in L^2(\Omega)^{2\times 2}.$$

Now we introduce a mixed Volterra formulation for the Reissner–Mindlin plate.

Problem 4.7. Given $(\boldsymbol{f}, g) \in L^\ell(\mathcal{J}; \boldsymbol{L}^2(\Omega) \times L^2(\Omega))$, find $(\boldsymbol{\theta}, w, \boldsymbol{\gamma}) \in L^\ell(\mathcal{J}; \boldsymbol{H}_0^1(\Omega) \times H_0^1(\Omega) \times \boldsymbol{L}^2(\Omega))$ such that

$$\begin{cases} a(\boldsymbol{\theta}, \boldsymbol{\eta}) + b((\boldsymbol{\eta}, v), \boldsymbol{\gamma}) = L(\boldsymbol{\eta}, v) + \displaystyle\int_0^t \dot{E}(t-s)[a(\boldsymbol{\theta}(s), \boldsymbol{\eta}) + b((\boldsymbol{\eta}, v), \boldsymbol{\gamma}(s))]\,\mathrm{d}s, \\ b((\boldsymbol{\theta}, w), \boldsymbol{q}) - \dfrac{d^2}{\kappa}(\boldsymbol{\gamma}, \boldsymbol{q}) = 0, \end{cases}$$

for all $(\boldsymbol{\eta}, v) \in \boldsymbol{H}_0^1(\Omega) \times H_0^1(\Omega)$ and for all $\boldsymbol{q} \in \boldsymbol{L}^2(\Omega)$, where $L(\boldsymbol{\eta}, v) := (g, v) - (\boldsymbol{f}, \boldsymbol{\eta})$.

Here, the bilinear forms $a : \boldsymbol{H}_0^1(\Omega) \times \boldsymbol{H}_0^1(\Omega) \to \mathbb{R}$ and $b : \boldsymbol{H}_0^1(\Omega) \times H_0^1(\Omega) \times \boldsymbol{L}^2(\Omega) \to \mathbb{R}$ are defined by

$$a(\boldsymbol{\theta}, \boldsymbol{\eta}) := (\mathbb{C}\boldsymbol{\varepsilon}(\boldsymbol{\theta}), \boldsymbol{\varepsilon}(\boldsymbol{\eta})), \qquad b((\boldsymbol{\eta}, v), \boldsymbol{q}) := (\boldsymbol{q}, \nabla v - \boldsymbol{\eta}).$$

Observe that the bilinear form $a(\cdot, \cdot)$ is elliptic due to Korn's inequality. Also, our framework suggests that $\mathcal{V} := \boldsymbol{H}_0^1(\Omega) \times H_0^1(\Omega)$ and $\mathcal{Q} := \boldsymbol{L}^2(\Omega)$. On the other hand, $b(\cdot, \cdot)$ does not satisfy an inf-sup condition in $\mathcal{Q}$ since the associated linear operator $\mathbb{B} : \mathcal{V} \to \mathcal{Q}'$, $\mathbb{B} : (\boldsymbol{\eta}, \psi) \to (\nabla\psi - \boldsymbol{\eta})$ is not surjective. According to Remark 10.4.4 from [8], one must consider $\mathcal{Q} = \boldsymbol{H}_0(\mathrm{rot}; \Omega)$ in order to satisfy an inf-sup condition, but that implies that the problem becomes into a *singular perturbation problem*, whose analysis is not covered with the present abstract framework.

4.2.1. Finite element discretization

The following numerical scheme is inspired by Durán and Liberman [16] and Section 6 of [19]. Let $\mathscr{T}_h$ be a regular family of triangulation of Ω. Let $\boldsymbol{H}_h, W_h, \boldsymbol{\Gamma}_h$ be finite element spaces associated with $\mathscr{T}_h$ such that

$$\boldsymbol{H}_h \subset \boldsymbol{H}_0^1(\Omega), \qquad W_h \subset H_0^1(\Omega), \qquad \boldsymbol{\Gamma}_h \subset \boldsymbol{L}^2(\Omega).$$

For efficient locking-free methods, the relation $\nabla W_h \subset \boldsymbol{\Gamma}_h$ is assumed. Let $\boldsymbol{\Pi}^{\boldsymbol{\Gamma}}$ be an interpolation operator mapping $\boldsymbol{H}_0^1(\Omega)$ to $\boldsymbol{\Gamma}_h$. Then, the corresponding finite element discretization of the viscoelastic Reissner–Mindlin plate is as follows.

Problem 4.8. Find $(\boldsymbol{\theta}_h, w_h, \boldsymbol{\gamma}_h) \in L^\ell(\mathcal{J}; \boldsymbol{H}_h \times W_h \times \boldsymbol{\Gamma}_h)$ such that given $(\boldsymbol{f}, g) \in L^\ell(\mathcal{J}; \boldsymbol{L}^2(\Omega) \times L^2(\Omega))$, we have

$$\begin{cases} a(\boldsymbol{\theta}_h, \boldsymbol{\eta}) + b((\boldsymbol{\eta}, v), \boldsymbol{\gamma}_h) = L(\boldsymbol{\eta}, v) + \displaystyle\int_0^t \dot{E}(t-s)[a(\boldsymbol{\theta}_h(s), \boldsymbol{\eta}) + b((\boldsymbol{\eta}, v), \boldsymbol{\gamma}_h(s))]\,\mathrm{d}s, \\ b((\boldsymbol{\theta}_h, w_h), \boldsymbol{q}) - \dfrac{d^2}{\kappa}(\boldsymbol{\gamma}_h, \boldsymbol{q}) = 0, \end{cases}$$

for all $(\boldsymbol{\eta}, v) \in \boldsymbol{H}_h \times W_h$ and for all $\boldsymbol{q} \in \boldsymbol{\Gamma}_h$.

The bilinear forms for this case are given by:

$$a(\boldsymbol{\theta}_h, \boldsymbol{\eta}) := (\mathbb{C}\boldsymbol{\varepsilon}(\boldsymbol{\theta}_h), \boldsymbol{\varepsilon}(\boldsymbol{\eta})), \qquad b((\boldsymbol{\theta}_h, v), \boldsymbol{q}) := \Big(\boldsymbol{q}, \nabla v - \boldsymbol{\Pi}^{\boldsymbol{\Gamma}}\boldsymbol{\theta}_h\Big).$$

Now we propose specific spaces for a locking-free method. We recall that Ω is assumed to be a convex polygonal domain. Let us denote by $\boldsymbol{E}$ and $\boldsymbol{n}$ the set of edges in the mesh $\mathscr{T}_h$ and the unit normal vector, respectively. We denote by M_k the space of piecewise polynomials of degree $\leq k$, and the corresponding vector-valued analogue by $\boldsymbol{M}_k := M_k \times M_k$. The Durán–Liberman element [16] corresponds to the choices

$$\boldsymbol{H}_h = \big\{\boldsymbol{\theta} \in \boldsymbol{M}_2 \cap \boldsymbol{H}_0^1 \,:\, \boldsymbol{\theta}\cdot\boldsymbol{n} \in \mathcal{P}_1(e),\, e \in \boldsymbol{E}\big\}, \quad W_h = M_1 \cap H_0^1, \quad \boldsymbol{\Gamma}_h = \boldsymbol{RT}_0^\perp,$$

where $\boldsymbol{RT}_0^\perp$ denotes the Raviart-Thomas discretization of the lowest order to $\boldsymbol{H}(\mathrm{rot})$. From this we take $\boldsymbol{\Pi}^{\boldsymbol{\Gamma}}$ as the usual interpolant into $\boldsymbol{RT}_0^\perp$, defined for $\boldsymbol{\gamma} \in \boldsymbol{H}^1(\Omega)$ by

$$\int_e \boldsymbol{\Pi}^{\boldsymbol{\Gamma}}\boldsymbol{\gamma}\cdot\boldsymbol{s} = \int_e \boldsymbol{\gamma}\cdot\boldsymbol{s}, \qquad e \in \boldsymbol{E}.$$

The choice of the aforementioned spaces and the interpolant $\boldsymbol{\Pi}^{\boldsymbol{\Gamma}}$ results in a locking-free scheme for the viscoelastic Reissner-Mindlin plate. The expected convergence rates should be similar to those of an elastic plate. We explore this in the next section.

4.2.2. Numerical tests.

Finally, we report a series of numerical tests in order to evaluate the accuracy of the scheme presented above for the viscoelastic plate problem. In order to continue with the uniformity of the experiments, the material selected is the same as the one used in the beam, *i.e.*, the SLS model. For this experiment we consider an observation time $T = 20\,\mathrm{s}$, with 5000 time steps. The plate domain is $\Omega = (0,1)^2$ and is assumed to be clamped in its whole boundary. The selected thickness are 10^{-3} m, 10^{-4} m and 10^{-5} m, with Poisson's ratio 0.3. For the numerical implementation, we wrote a FEniCS code. The reduction operator was obtained with the help of FEniCS-shells [25]. The quasi-static analytical solution is derived from [14] and the correspondence principle. For instance, we have

$$w(x,y,t) = J(t)\tilde{w}(x,y), \quad \beta_1(x,y,t) = J(t)\tilde{\beta}_1(x,y), \quad \beta_2(x,y,t) = J(t)\tilde{\beta}_2(x,y),$$

where $J(t)$ is the creep compliance [37], and

$$\begin{aligned} \tilde{w}(x,y) &= \frac{1}{3}x^3(x-1)^3y^3(y-1)^3 - \frac{2d^2}{5(1-\nu)}\big[y^3(y-1)^3x(x-1)\big(5x^2-5x+1\big) \\ &\quad + x^3(x-1)^3y(y-1)\big(5y^2-5y+1\big)\big], \\ \tilde{\theta}_1(x,y) &= y^3(y-1)^3x^2(x-1)^2(2x-1), \\ \tilde{\theta}_2(x,y) &= x^3(x-1)^3y^2(y-1)^2(2y-1). \end{aligned}$$

Tables 6–10 show the behavior of the error when is computed with different values of ℓ with respect to the energy norm and the usual L^2 norm. Since the time step is one order of magnitude smaller than the smallest mesh size considered, there is no influence on the choice of ℓ. Similar to the beam case, the experimental

TABLE 6. Computed error values in $L^2(\Omega)$ and experimental rates of convergence of the transverse displacement w in a fully clamped viscoelastic Reissner–Mindlin plate.

		$d = 10^{-3}$ m		$d = 10^{-4}$ m		$d = 10^{-5}$ m	
DOF	h	$\mathtt{e}_{0,1}(w)$	$\mathtt{r}_{0,1}(w)$	$\mathtt{e}_{0,1}(w)$	$\mathtt{r}_{0,1}(w)$	$\mathtt{e}_{0,1}(w)$	$\mathtt{r}_{0,1}(w)$
1323	0.141	9.6331e−02	–	9.6326e−02	–	9.6326e−02	–
2883	0.094	4.0489e−02	2.14	4.0474e−02	2.14	4.0473e−02	2.14
5043	0.071	2.1939e−02	2.13	2.1918e−02	2.13	2.1917e−02	2.13
7803	0.057	1.3704e−02	2.11	1.3678e−02	2.11	1.3678e−02	2.11
11163	0.047	9.3621e−03	2.09	9.3344e−03	2.10	9.3341e−03	2.10
15123	0.040	6.8005e−03	2.07	6.7710e−03	2.08	6.7707e−03	2.08
DOF	h	$\mathtt{e}_{0,2}(w)$	$\mathtt{r}_{0,2}(w)$	$\mathtt{e}_{0,2}(w)$	$\mathtt{r}_{0,2}(w)$	$\mathtt{e}_{0,2}(w)$	$\mathtt{r}_{0,2}(w)$
1323	0.141	9.6331e−02	–	9.6326e−02	–	9.6326e−02	–
2883	0.094	4.0489e−02	2.14	4.0474e−02	2.14	4.0474e−02	2.14
5043	0.071	2.1939e−02	2.13	2.1918e−02	2.13	2.1917e−02	2.13
7803	0.057	1.3704e−02	2.11	1.3678e−02	2.11	1.3678e−02	2.11
11163	0.047	9.3621e−03	2.09	9.3344e−03	2.10	9.3341e−03	2.10
15123	0.040	6.8005e−03	2.07	6.7710e−03	2.08	6.7707e−03	2.08
DOF	h	$\mathtt{e}_{0,\infty}(w)$	$\mathtt{r}_{0,\infty}(w)$	$\mathtt{e}_{0,\infty}(w)$	$\mathtt{r}_{0,\infty}(w)$	$\mathtt{e}_{0,\infty}(w)$	$\mathtt{r}_{0,\infty}(w)$
1323	0.141	9.6331e−02	–	9.6326e−02	–	9.6326e−02	–
2883	0.094	4.0489e−02	2.14	4.0474e−02	2.14	4.0473e−02	2.14
5043	0.071	2.1939e−02	2.13	2.1917e−02	2.13	2.1917e−02	2.13
7803	0.057	1.3703e−02	2.11	1.3678e−02	2.11	1.3678e−02	2.11
11163	0.047	9.3620e−03	2.09	9.3343e−03	2.10	9.3340e−03	2.10
15123	0.040	6.8004e−03	2.07	6.7709e−03	2.08	6.7706e−03	2.08

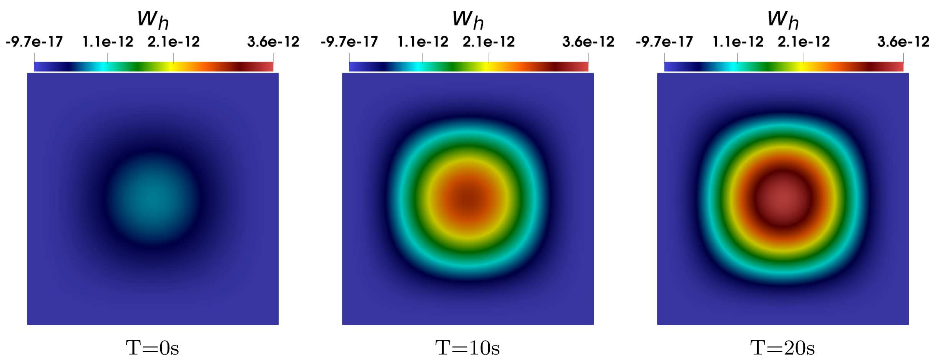

FIGURE 2. Evolution of the viscoelastic displacement w_h in the fully clamped plate, where $d = 10^{-5}$ m and $\Delta t = 0.004$.

convergence orders are optimal, coinciding with those obtained in elastic plates in [16, 19]. This, together with the low number of degrees of freedom used, shows that the method is locking-free. In Figures 2 and 3, we present the evolution of the transverse displacement w_h and the components of the rotation vector $\boldsymbol{\theta}_h = (\theta_{1h}, \theta_{2h})$ at different times steps to verify that the method takes into account the presence of the creep compliance, typical of the SLS material.

We end this section reporting the creep compliance for w and w_h in the center of the plate, *i.e.*, the point of maximum deflection. In Figure 4, the bounded creep behavior is clearly visible, and also, is observable how the viscoelastic discrete and exact solution match almost exactly.

TABLE 7. Computed error values in $\boldsymbol{L}^2(\Omega)$ and experimental rates of convergence of the rotation $\boldsymbol{\theta}$ in a fully clamped viscoelastic Reissner–Mindlin plate.

		$d=10^{-3}$ m		$d=10^{-4}$ m		$d=10^{-5}$ m	
DOF	h	$\mathtt{e}_{\mathbf{0},1}(\boldsymbol{\theta})$	$\mathtt{r}_{\mathbf{0},1}(\boldsymbol{\theta})$	$\mathtt{e}_{\mathbf{0},1}(\boldsymbol{\theta})$	$\mathtt{r}_{\mathbf{0},1}(\boldsymbol{\theta})$	$\mathtt{e}_{\mathbf{0},1}(\boldsymbol{\theta})$	$\mathtt{r}_{\mathbf{0},1}(\boldsymbol{\theta})$
1323	0.141	9.6230e−02	–	9.6232e−02	–	9.6232e−02	–
2883	0.094	4.1107e−02	2.10	4.1102e−02	2.10	4.1102e−02	2.10
5043	0.071	2.2532e−02	2.09	2.2522e−02	2.09	2.2522e−02	2.09
7803	0.057	1.4185e−02	2.07	1.4173e−02	2.08	1.4173e−02	2.08
11163	0.047	9.7444e−03	2.06	9.7313e−03	2.06	9.7312e−03	2.06
15123	0.040	7.1065e−03	2.05	7.0924e−03	2.05	7.0923e−03	2.05
DOF	h	$\mathtt{e}_{\mathbf{0},2}(\boldsymbol{\theta})$	$\mathtt{r}_{\mathbf{0},2}(\boldsymbol{\theta})$	$\mathtt{e}_{\mathbf{0},2}(\boldsymbol{\theta})$	$\mathtt{r}_{\mathbf{0},2}(\boldsymbol{\theta})$	$\mathtt{e}_{\mathbf{0},2}(\boldsymbol{\theta})$	$\mathtt{r}_{\mathbf{0},2}(\boldsymbol{\theta})$
1323	0.141	9.6231e−02	–	9.6232e−02	–	9.6232e−02	–
2883	0.094	4.1107e−02	2.10	4.1102e−02	2.10	4.1102e−02	2.10
5043	0.071	2.2532e−02	2.09	2.2522e−02	2.09	2.2522e−02	2.09
7803	0.057	1.4185e−02	2.07	1.4173e−02	2.08	1.4173e−02	2.08
11163	0.047	9.7444e−03	2.06	9.7313e−03	2.06	9.7312e−03	2.06
15123	0.040	7.1065e−03	2.05	7.0924e−03	2.05	7.0923e−03	2.05
DOF	h	$\mathtt{e}_{\mathbf{0},\infty}(\boldsymbol{\theta})$	$\mathtt{r}_{\mathbf{0},\infty}(\boldsymbol{\theta})$	$\mathtt{e}_{\mathbf{0},\infty}(\boldsymbol{\theta})$	$\mathtt{r}_{\mathbf{0},\infty}(\boldsymbol{\theta})$	$\mathtt{e}_{\mathbf{0},\infty}(\boldsymbol{\theta})$	$\mathtt{r}_{\mathbf{0},\infty}(\boldsymbol{\theta})$
1323	0.141	9.6230e−02	–	9.6232e−02	–	9.6232e−02	–
2883	0.094	4.1107e−02	2.10	4.1102e−02	2.10	4.1102e−02	2.10
5043	0.071	2.2532e−02	2.09	2.2522e−02	2.09	2.2522e−02	2.09
7803	0.057	1.4184e−02	2.07	1.4173e−02	2.08	1.4173e−02	2.08
11163	0.047	9.7443e−03	2.06	9.7312e−03	2.06	9.7311e−03	2.06
15123	0.040	7.1064e−03	2.05	7.0923e−03	2.05	7.0922e−03	2.05

TABLE 8. Computed error values in $\boldsymbol{L}^2(\Omega)$ and experimental rates of convergence of the rotation $\boldsymbol{\gamma}$ in a fully clamped viscoelastic Reissner–Mindlin plate.

		$d=10^{-3}$ m		$d=10^{-4}$ m		$d=10^{-5}$ m	
DOF	h	$\mathtt{e}_{\mathbf{0},1}(\boldsymbol{\gamma})$	$\mathtt{r}_{\mathbf{0},1}(\boldsymbol{\gamma})$	$\mathtt{e}_{\mathbf{0},1}(\boldsymbol{\gamma})$	$\mathtt{r}_{\mathbf{0},1}(\boldsymbol{\gamma})$	$\mathtt{e}_{\mathbf{0},1}(\boldsymbol{\gamma})$	$\mathtt{r}_{\mathbf{0},1}(\boldsymbol{\gamma})$
1323	0.141	3.7369e−01	–	3.7369e−01	–	3.7369e−01	–
2883	0.094	2.5115e−01	0.98	2.5115e−01	0.98	2.5115e−01	0.98
5043	0.071	1.8875e−01	0.99	1.8875e−01	0.99	1.8875e−01	0.99
7803	0.057	1.5106e−01	1.00	1.5106e−01	1.00	1.5106e−01	1.00
11163	0.047	1.2587e−01	1.00	1.2587e−01	1.00	1.2587e−01	1.00
15123	0.040	1.0787e−01	1.00	1.0787e−01	1.00	1.0787e−01	1.00
DOF	h	$\mathtt{e}_{\mathbf{0},2}(\boldsymbol{\gamma})$	$\mathtt{r}_{\mathbf{0},2}(\boldsymbol{\gamma})$	$\mathtt{e}_{\mathbf{0},2}(\boldsymbol{\gamma})$	$\mathtt{r}_{\mathbf{0},2}(\boldsymbol{\gamma})$	$\mathtt{e}_{\mathbf{0},2}(\boldsymbol{\gamma})$	$\mathtt{r}_{\mathbf{0},2}(\boldsymbol{\gamma})$
1323	0.141	3.7369e−01	–	3.7369e−01	–	3.7369e−01	–
2883	0.094	2.5115e−01	0.98	2.5115e−01	0.98	2.5115e−01	0.98
5043	0.071	1.8875e−01	0.99	1.8875e−01	0.99	1.8875e−01	0.99
7803	0.057	1.5106e−01	1.00	1.5106e−01	1.00	1.5106e−01	1.00
11163	0.047	1.2587e−01	1.00	1.2587e−01	1.00	1.2587e−01	1.00
15123	0.040	1.0787e−01	1.00	1.0787e−01	1.00	1.0787e−01	1.00
DOF	h	$\mathtt{e}_{\mathbf{0},\infty}(\boldsymbol{\gamma})$	$\mathtt{r}_{\mathbf{0},\infty}(\boldsymbol{\gamma})$	$\mathtt{e}_{\mathbf{0},\infty}(\boldsymbol{\gamma})$	$\mathtt{r}_{\mathbf{0},\infty}(\boldsymbol{\gamma})$	$\mathtt{e}_{\mathbf{0},\infty}(\boldsymbol{\gamma})$	$\mathtt{r}_{\mathbf{0},\infty}(\boldsymbol{\gamma})$
1323	0.141	3.7369e−01	–	3.7369e−01	–	3.7369e−01	–
2883	0.094	2.5115e−01	0.98	2.5115e−01	0.98	2.5115e−01	0.98
5043	0.071	1.8875e−01	0.99	1.8875e−01	0.99	1.8875e−01	0.99
7803	0.057	1.5106e−01	1.00	1.5106e−01	1.00	1.5106e−01	1.00
11163	0.047	1.2587e−01	1.00	1.2587e−01	1.00	1.2587e−01	1.00
15123	0.040	1.0787e−01	1.00	1.0787e−01	1.00	1.0787e−01	1.00

TABLE 9. Computed error values in $H^1(\Omega)$ and experimental rates of convergence of the transverse displacement w in a fully clamped viscoelastic Reissner–Mindlin plate.

		$d = 10^{-3}$ m		$d = 10^{-4}$ m		$d = 10^{-5}$ m	
DOF	h	$\mathtt{e}_{1,1}(w)$	$\mathtt{r}_{1,1}(w)$	$\mathtt{e}_{1,1}(w)$	$\mathtt{r}_{1,1}(w)$	$\mathtt{e}_{1,1}(w)$	$\mathtt{r}_{1,1}(w)$
1323	0.141	2.4308e−01	–	2.4308e−01	–	2.4308e−01	–
2883	0.094	1.5965e−01	1.04	1.5965e−01	1.04	1.5965e−01	1.04
5043	0.071	1.1919e−01	1.02	1.1919e−01	1.02	1.1919e−01	1.02
7803	0.057	9.5166e−02	1.01	9.5164e−02	1.01	9.5164e−02	1.01
11163	0.047	7.9227e−02	1.01	7.9226e−02	1.01	7.9226e−02	1.01
15123	0.040	6.7871e−02	1.00	6.7869e−02	1.00	6.7869e−02	1.00
DOF	h	$\mathtt{e}_{1,2}(w)$	$\mathtt{r}_{1,2}(w)$	$\mathtt{e}_{1,2}(w)$	$\mathtt{r}_{1,2}(w)$	$\mathtt{e}_{1,2}(w)$	$\mathtt{r}_{1,2}(w)$
1323	0.141	2.4308e−01	–	2.4308e−01	–	2.4308e−01	–
2883	0.094	1.5965e−01	1.04	1.5965e−01	1.04	1.5965e−01	1.04
5043	0.071	1.1919e−01	1.02	1.1919e−01	1.02	1.1919e−01	1.02
7803	0.057	9.5166e−02	1.01	9.5164e−02	1.01	9.5164e−02	1.01
11163	0.047	7.9227e−02	1.01	7.9226e−02	1.01	7.9226e−02	1.01
15123	0.040	6.7871e−02	1.00	6.7869e−02	1.00	6.7869e−02	1.00
DOF	h	$\mathtt{e}_{1,\infty}(w)$	$\mathtt{r}_{1,\infty}(w)$	$\mathtt{e}_{1,\infty}(w)$	$\mathtt{r}_{1,\infty}(w)$	$\mathtt{e}_{1,\infty}(w)$	$\mathtt{r}_{1,\infty}(w)$
1323	0.141	2.4308e−01	–	2.4308e−01	–	2.4308e−01	–
2883	0.094	1.5965e−01	1.04	1.5965e−01	1.04	1.5965e−01	1.04
5043	0.071	1.1919e−01	1.02	1.1919e−01	1.02	1.1919e−01	1.02
7803	0.057	9.5166e−02	1.01	9.5164e−02	1.01	9.5164e−02	1.01
11163	0.047	7.9227e−02	1.01	7.9226e−02	1.01	7.9226e−02	1.01
15123	0.040	6.7871e−02	1.00	6.7869e−02	1.00	6.7869e−02	1.00

TABLE 10. Computed error values in $\boldsymbol{H}^1(\Omega)$ and experimental rates of convergence of the rotation $\boldsymbol{\theta}$ in a fully clamped viscoelastic Reissner–Mindlin plate.

		$d = 10^{-3}$ m		$d = 10^{-4}$ m		$d = 10^{-5}$ m	
DOF	h	$\mathtt{e}_{1,1}(\boldsymbol{\theta})$	$\mathtt{r}_{1,1}(\boldsymbol{\theta})$	$\mathtt{e}_{1,1}(\boldsymbol{\theta})$	$\mathtt{r}_{1,1}(\boldsymbol{\theta})$	$\mathtt{e}_{1,1}(\boldsymbol{\theta})$	$\mathtt{r}_{1,1}(\boldsymbol{\theta})$
1323	0.141	3.3783e−01	–	3.3784e−01	–	3.3784e−01	–
2883	0.094	2.3897e−01	0.85	2.3896e−01	0.85	2.3896e−01	0.85
5043	0.071	1.8480e−01	0.89	1.8479e−01	0.89	1.8479e−01	0.89
7803	0.057	1.5080e−01	0.91	1.5078e−01	0.91	1.5078e−01	0.91
11163	0.047	1.2746e−01	0.92	1.2744e−01	0.92	1.2744e−01	0.92
15123	0.040	1.1043e−01	0.93	1.1041e−01	0.93	1.1041e−01	0.93
DOF	h	$\mathtt{e}_{1,2}(\boldsymbol{\theta})$	$\mathtt{r}_{1,2}(\boldsymbol{\theta})$	$\mathtt{e}_{1,2}(\boldsymbol{\theta})$	$\mathtt{r}_{1,2}(\boldsymbol{\theta})$	$\mathtt{e}_{1,2}(\boldsymbol{\theta})$	$\mathtt{r}_{1,2}(\boldsymbol{\theta})$
1323	0.141	3.3783e−01	–	3.3784e−01	–	3.3784e−01	–
2883	0.094	2.3897e−01	0.85	2.3896e−01	0.85	2.3896e−01	0.85
5043	0.071	1.8480e−01	0.89	1.8479e−01	0.89	1.8479e−01	0.89
7803	0.057	1.5080e−01	0.91	1.5078e−01	0.91	1.5078e−01	0.91
11163	0.047	1.2746e−01	0.92	1.2744e−01	0.92	1.2744e−01	0.92
15123	0.040	1.1043e−01	0.93	1.1041e−01	0.93	1.1041e−01	0.93
DOF	h	$\mathtt{e}_{1,\infty}(\boldsymbol{\theta})$	$\mathtt{r}_{1,\infty}(\boldsymbol{\theta})$	$\mathtt{e}_{1,\infty}(\boldsymbol{\theta})$	$\mathtt{r}_{1,\infty}(\boldsymbol{\theta})$	$\mathtt{e}_{1,\infty}(\boldsymbol{\theta})$	$\mathtt{r}_{1,\infty}(\boldsymbol{\theta})$
1323	0.141	3.3783e−01	–	3.3784e−01	–	3.3784e−01	–
2883	0.094	2.3897e−01	0.85	2.3896e−01	0.85	2.3896e−01	0.85
5043	0.071	1.8480e−01	0.89	1.8479e−01	0.89	1.8479e−01	0.89
7803	0.057	1.5080e−01	0.91	1.5078e−01	0.91	1.5078e−01	0.91
11163	0.047	1.2746e−01	0.92	1.2744e−01	0.92	1.2744e−01	0.92
15123	0.040	1.1043e−01	0.93	1.1041e−01	0.93	1.1041e−01	0.93

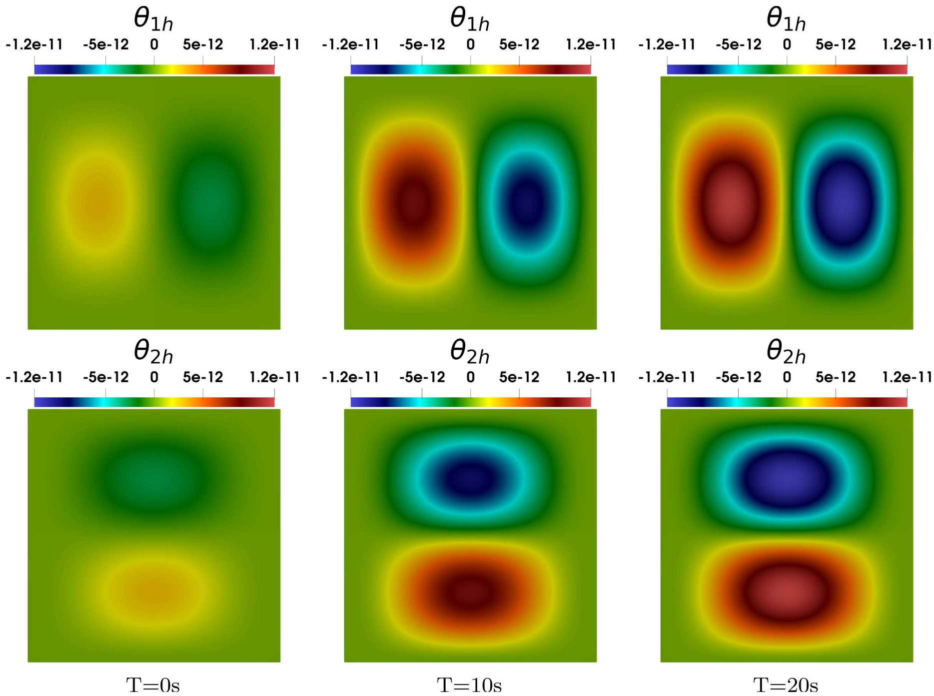

FIGURE 3. Evolution of the viscoelastic rotation components β_{ih} in the fully clamped, where $d = 10^{-5}$ m and $\Delta t = 0.04$.

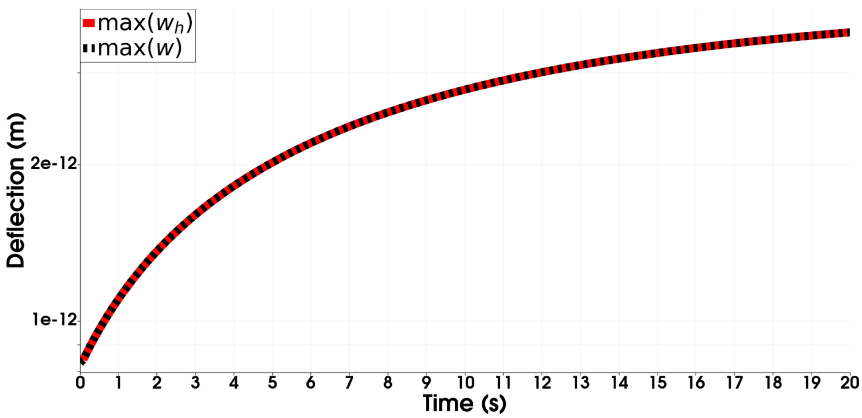

FIGURE 4. Comparison between the exact and discrete maximum transverse displacement in the viscoelastic Reissner–Mindlin plate, where $d = 10^{-5}$ m and $\Delta t = 0.04$.

5. CONCLUSIONS

We have presented an abstract functional framework to deal with mixed formulations for viscoelastic problems, where perturbations parameters arise. We have shown the solvability of mixed viscoelastic formulations, adapting the well known theory for elliptic mixed formulations. The relevance is focused in the independence of the perturbation parameter in every estimate, since in the applications, numerical methods can be affected, deteriorating the stability and convergence. With the well established theory of Volterra equations, we have proved convergence of mixed conforming numerical methods for the mixed viscoelastic problem, where the convergence is independent of the perturbation parameter.

The application that we performed, for Timoshenko beams, confirms that the proposed abstract framework is suitable for slender structures, where the thickness parameter do not produces difficulties for numerical methods, when viscoelastic materials are considered. Also, the numerical experimentation with the Reissner–Mindlin plate provides data that allows us to infer that a viscoelastic mixed analysis can be performed, with the corresponding theoretical extensions that are needed. This is an ongoing analysis and will be the subject of forthcoming papers.

Acknowledgements. Erwin Hernández has been partially supported by FONDECYT project No. 1181098, Chile. Felipe Lepe has been partially supported by DIUBB through project 2120173 GI/C Universidad del Bío-Bío and FONDECYT project No. 11200529, Chile. Jesus Vellojin has been partially supported by the National Agency for Research and Development, ANID-Chile through project Anillo of Computational Mathematics for Desalination Processes ACT210087, FONDECYT Postdoctorado project 3230302, and by project Centro de Modelamiento Matemático (CMM), FB210005, BASAL funds for centers of excellence.

References

[1] M.S. Alnæs, J. Blechta, J. Hake, A. Johansson, B. Kehlet, A. Logg, C. Richardson, J. Ring, M.E. Rognes and G.N. Wells, The FEniCS project version 1.5. *Arch. Numer. Software* **3** (2015) 9–23.

[2] H. Aminikhah and J. Biazar, A new analytical method for solving systems of Volterra integral equations. *Int. J. Comput. Math.* **87** (2010) 1142–1157.

[3] J. Argyris, I. St. Doltsinis and V.D. da silva, Constitutive modelling and computation of non-linear viscoelastic solids. Part I: rheological models and numerical integration techniques. *Comput. Methods Appl. Mech. Eng.* **88** (1991) 135–163.

[4] D.N. Arnold, Discretization by finite elements of a model parameter dependent problem. *Numer. Math.* **37** (1981) 405–421.

[5] H.T. Banks, S. Hu and Z.R. Kenz, A brief review of elasticity and viscoelasticity for solids. *Adv. Appl. Math. Mech.* **3** (2011) 1–51.

[6] K.J. Bathe, Finite Element Procedures. Prentice-Hall (1996).

[7] L. Beirão da Veiga, D. Mora and G. Rivera, Virtual elements for a shear-deflection formulation of Reissner–Mindlin plates. *Math. Comp.* **88** (2019) 149–178.

[8] D. Boffi, F. Brezzi and M. Fortin, Mixed Finite Element Methods and Applications. Vol. 44, Springer (2013).

[9] D. Chapelle, A locking-free approximation of curved rods by straight beam elements. *Numer. Math.* **77** (1997) 299–322.

[10] D. Chapelle and K.-J. Bathe, The Finite Element Analysis of Shells-Fundamentals. Springer Science & Business Media (2013).

[11] T.-M. Chen, The hybrid laplace transform/finite element method applied to the quasi-static and dynamic analysis of viscoelastic Timoshenko beams. *Int. J. Numer. Methods Eng.* **38** (1995) 509–522.

[12] Q. Chen and Y.W. Chan, Integral finite element method for dynamical analysis of elastic–viscoelastic composite structures. *Comput. Struct.* **74** (2000) 51–64.

[13] G. Chen, X. Xie, Y. Xu and Y. Zhang, A locking-free stabilized embedded discontinuous Galerkin method for linear elasticity with strong symmetric stress and continuous displacement trace approximation. *Comput. Math. Appl.* **134** (2023) 66–86.

[14] C. Chinosi and C. Lovadina, Numerical analysis of some mixed finite element methods for Reissner–Mindlin plates. *Comput. Mech.* **16** (1995) 36–44.

[15] R. Christensen, Theory of Viscoelasticity: An Introduction. Elsevier (2012).

[16] R. Durán and E. Liberman, On mixed finite element methods for the Reissner–Mindlin plate model. *Math. Comput.* **58** (1992) 561–573.

[17] A. Ern and J.-L. Guermond, Theory and Practice of Finite Elements. Vol. 159. Springer Science & Business Media (2013).

[18] R.E. Ewing, Y. Lin, T. Sun, J. Wang and S. Zhang, Sharp l 2-error estimates and superconvergence of mixed finite element methods for non-fickian flows in porous media. *SIAM J. Numer. Anal.* **40** (2002) 1538–1560.

[19] R.S. Falk, Finite elements for the Reissner–Mindlin plate, in Mixed Finite Elements, Compatibility Conditions, and Applications. Springer (2008) 195–232.

[20] W. Flügge, Viscoelasticity. Springer-Verlag, Berlin Google Scholar (1975).

[21] T. Führer, C. García Vera and N. Heuer, A locking-free DPG scheme for Timoshenko beams. *Comput. Methods Appl. Math.* **21** (2021) 373–383.

[22] J.M. Golden and G.A.C. Graham, Boundary Value Problems in Linear Viscoelasticity. Springer Science & Business Media (2013).

[23] G. Gripenberg, S.-O. Londen and O. Staffans, Volterra Integral and Functional Equations. Vol. 34. Cambridge University Press (1990).

[24] D. Gutierrez-Lemini, Engineering Viscoelasticity. Springer (2014).

[25] J.S. Hale, M. Brunetti, S.P.A. Bordas and C. Maurini, FEniCS-Shells (2016).

[26] G. Harper, R. Wang, J. Liu, S. Tavener and R. Zhang, A locking-free solver for linear elasticity on quadrilateral and hexahedral meshes based on enrichment of Lagrangian elements. *Comput. Math. Appl.* **80** (2020) 1578–1595.

[27] E. Hernández and J. Vellojin, A locking-free finite element formulation for a non-uniform linear viscoelastic Timoshenko beam. *Comput. Math. App.* **99** (2021) 305–322.

[28] E. Hernandez, C. Naranjo and J. Vellojin, Modelling of thin viscoelastic shell structures under Reissner–Mindlin kinematic assumption. *Appl. Math. Modell.* **79** (2020) 180–199.

[29] V. Janovský, S. Shaw, M.K. Warby and J.R. Whiteman, Numerical methods for treating problems of viscoelastic isotropic solid deformation. *J. Comput. Appl. Math.* **63** (1995) 91–107.

[30] S. Karaa and A.K. Pani, Optimal error estimates of mixed fems for second order hyperbolic integro-differential equations with minimal smoothness on initial data. *J. Comput. Appl. Math.* **275** (2015) 113–134.

[31] S. Lee and S.-Y. Yi, Locking-free and locally-conservative enriched Galerkin method for poroelasticity. *J. Sci. Comput.* **94** (2023) 23.

[32] F. Lepe, D. Mora and R. Rodríguez, Locking-free finite element method for a bending moment formulation of Timoshenko beams. *Comput. Math. App.* **68** (2014) 118–131.

[33] F. Lepe, D. Mora and R. Rodríguez, Finite element analysis of a bending moment formulation for the vibration problem of a non-homogeneous Timoshenko beam. *J. Sci. Comput.* **66** (2016) 825–848.

[34] S.-O. Londen, On an integral equation in a Hilbert space. *SIAM J. Math. Anal.* **8** (1977) 950–970.

[35] C. Lovadina, D. Mora and R. Rodríguez, Approximation of the buckling problem for Reissner–Mindlin plates. *SIAM J. Numer. Anal.* **48** (2010) 603–632.

[36] C. Lovadina, D. Mora and R. Rodríguez, A locking-free finite element method for the buckling problem of a non-homogeneous Timoshenko beam. *ESAIM: Math. Model. Numer. Anal.* **45** (2011) 603–626.

[37] O. Martin, Quasi-static and dynamic analysis for viscoelastic beams with the constitutive equation in a hereditary integral form. *Ann. Univ. Bucharest* **5** (2014) 1–13.

[38] O. Martin, A modified variational iteration method for the analysis of viscoelastic beams. *Appl. Math. Modell.* **40** (2016) 7988–7995.

[39] C.C. Miao and S. Tsimin, Finite Element Methods for Integrodifferential Equations. Vol. 9. World Scientific (1998).

[40] S. Mukherjee and G.H. Paulino, The elastic-viscoelastic correspondence principle for functionally graded materials, revisited. *J. Appl. Mech.* **70** (2003) 359–363.

[41] G.S. Payette and J.N. Reddy, Nonlinear quasi-static finite element formulations for viscoelastic Euler-Bernoulli and Timoshenko beams. *Int. J. Numer. Methods Biomed. Eng.* **26** (2010) 1736–1755.

[42] G.S. Payette and J.N. Reddy, A nonlinear finite element framework for viscoelastic beams based on the high-order reddy beam theory. *J. Eng. Mater. Technol.* **135** (2013) 011005.

[43] J.N. Reddy, An Introduction to Continuum Mechanics. Cambridge University Press (2007).

[44] M. Rognes and R. Winther, Mixed finite element methods for linear viscoelasticity using weak symmetry. *Math. Models Methods Appl. Sci. – M3AS* **20** (2010) 955–985.

[45] F. Saedpanah, Existence and convergence of galerkin approximation for second order hyperbolic equations with memory term. *Numer. Methods Part. Differ. Equ.* **32** (2016) 548–563.

[46] S. Shaw and J.R. Whiteman, Optimal long-time $L_p(0,T)$ stability and semidiscrete error estimates for the Volterra formulation of the linear quasistatic viscoelasticity problem. *Numer. Math.* **88** (2001) 743–770.

[47] J.C. Simo and T.J.R. Hughes, Computational inelasticity. Vol. 7. Springer Science & Business Media (2006).

[48] R.K. Sinha, R.E. Ewing and R.D. Lazarov, Mixed finite element approximations of parabolic integro-differential equations with nonsmooth initial data. *SIAM J. Numer. Anal.* **47** (2009) 3269–3292.

[49] D.W. Van Krevelen and K. Te Nijenhuis, Properties of Polymers: Their Correlation with Chemical Structure; Their Numerical Estimation and Prediction from Additive Group Contributions. Elsevier (2009).

[50] Z. Zheng-You, L. Gen-Guo and C. Chang-Jun, Quasi-static and dynamical analysis for viscoelastic Timoshenko beam with fractional derivative constitutive relation. *Appl. Math. Mech.* **23** (2002) 1–12.